Supporting Information

For

Carrier Protein Mediated Cargo Sensing in Quorum Signal Synthases

Patrick D. Fischer[1,3,4], Abu Sayeed Chowdhury[6], Thomas Bartholow[5], Shibani Basu[2], Eric Baggs[2], Huel S. Cox[1,3], Srđan Matošin[1,3], Michael D. Burkart[5], Lisa Warner[2], Rajesh Nagarajan[2*] and Haribabu Arthanari[1*]

[1] Department of Biological Chemistry and Molecular Pharmacology, Harvard Medical School, Boston, MA, USA.
[2] Department of Chemistry and Biochemistry, Boise State University, Boise, ID, USA.
[3] Department of Cancer Biology, Dana-Farber Cancer Institute, Boston, MA, USA.
[4] Department of Pharmacy, Pharmaceutical and Medicinal Chemistry, Saarland University, Saarbrucken, Germany.
[5] Department of Chemistry and Biochemistry, University of California, San Diego, CA, USA.
[6] Biomolecular Sciences Graduate Program, Boise State University, Boise, ID, USA

*Corresponding authors: hari_arthanari@hms.harvard.edu; rajnagarajan@boisestate.edu

Contents

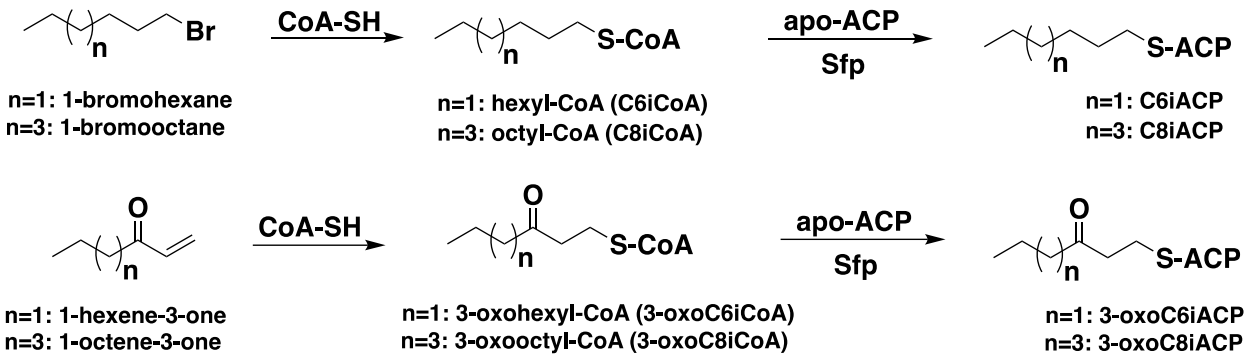

Scheme S1. Synthetic Scheme for alkyl-ACPs.

General Information

All chemical reagents and solvents were purchased from commercial sources and used without further purification, except where indicated. The alkyl-CoA compounds were synthesized using scheme S1. Size exclusion chromatography was performed using a NGC Quest 10 Plus FPLC system (Bio-Rad). A Thermo Scientific Evolution 260 Bio UV-Vis spectrophotometer was used to measure the concentration of analytes. HPLC data was analyzed by Chromeleon 7.2 software on a Thermo Scientific Dionex UltiMate-3000 HPLC system. Thermo Scientific Hypersil Gold C18 reverse-phase analytical UHPLC column (25002-054630) and semipreparative HPLC column (25005-159070) were used in alkyl-ACP and alkyl-CoA syntheses, respectively. Deuterated solvents, ^{15}N ammonium chloride and ^{13}C glucose were obtained commercially through Cambridge Isotope Laboratories, Inc. The isotopes for ACP_b purification were purchased from Millipore Sigma (Burlington, MA). Unless otherwise noted, all reagents were purchased from Fisher Scientific (Waltham, MA). Chemical shifts were expressed in parts per million (ppm) and referenced to residual solvent as the internal reference for ^{1}H ($CDCl_3$: δ = 7.24 ppm or CD_3OD: δ = 3.31 ppm) and ^{13}C ($CDCl_3$: δ = 77.16 ppm and CD_3OD: δ = 49.00 ppm). We are grateful to the following PI's for providing plasmids for the following proteins: *Pantoea Stewartii* EsaI (Prof. Mair Churchill, University of Colorado-Denver), *Burkholderia mallei* BmaI1 (Prof. E. P. Greenberg, University of Washington-Seattle) and *Escherichia coli* ACP (Prof. John Cronan, University of Illinois-Urbana Champaign).

General procedure for alkyl-CoA synthesis.

To a 1 mL aqueous solution of CoA-SH (65 μmol) in about 6 mg potassium carbonate (until the pH reached between 8-9), 30 μmol (19 mg) TCEP, 1 mL DMF, 120 μmol of 1-bromoalkane (1-bromohexane for C6iCoA, 1-bromooctane for C8iCoA) or alkylvinylketone (1-hexen-3-one for 3-oxoC6iCoA, 1-octen-3-one for 3-oxoC8iCoA) was added and the reaction mixture was stirred in nitrogen overnight.[1-3] Reaction completion was checked for absence of free thiol using sodium nitroprusside. The mixture was then diluted with 3 mL nanopure water and extracted thrice with 5 ml diethyl ether, to remove the unreacted alkyl bromide. The aqueous layer was filtered with 0.2 μm filter and loaded on to a semi-prep C18 HPLC column. Alkyl-CoA peak was collected using a 25 mM ammonium acetate (pH-5) in water and acetonitrile gradient system (both solvents in 0.1% trifluoroacetic acid) where the percent acetonitrile was gradually increased from 5% to 70% over a period of 10 minutes with a flow rate of 3 mL/min. Alkyl-CoA solution was then flushed with nitrogen to remove acetonitrile from the HPLC solvent. The solution was lyophilized and stored at -80 ºC until further use.

Mass determination of alkyl-CoA compounds. Alkyl-CoA compounds were characterized on an ultra-high resolution Bruker maXis Quadrupole Time of Flight (QTOF) instrument using direct injection to the MS. The ESI source was operated under the following conditions: positive ion mode, nebulizer pressure: 0.4 Bar; flow rate of drying gas (N_2): 4L/min; drying gas temperature: 200 ºC; voltage between HV capillary and HV end-plate offset: 3000 V to -500 V; and the quadrupole ion energy was 4.0 eV. Sodium formate was used to calibrate the

system in the mass range. All MS data was analyzed using the Compass Data Analysis software package (Bruker Corporation, Billerica, Massachusetts).

Hexyl-CoA (C6iCoA) HRMS (ESI-TOF) *m/z* calculated for $[M+H]^+$: 852.2163, observed: 852.2203.

Octyl-CoA (C8iCoA) HRMS (ESI-TOF) *m/z* calculated for $[M+H]^+$: 880.2476, observed: 880.2533.

3-oxohexyl-CoA (3-oxoC6iCoA) HRMS (ESI-TOF) *m/z* calculated for $[M+H]^+$: 866.1956, observed: 866.1953.

3-oxooctyl-CoA (3-oxoC8iCoA) HRMS (ESI-TOF) *m/z* calculated for $[M+H]^+$: 894.2269, observed: 894.2248.

Expression of proteins.

ACP from *E. coli* was expressed using a construct and bacterial strain designed by CRONAN and THOMAS.[4] They used the *E. coli* K-12 strain DK574[5], which is strain SJ16[6], bearing a pJT94 plasmid encoding ACP hydrolase (ACPH) under *lac* promoter control. BmaI1 and EsaI were expressed using His6-tagged constructs in pET expression vectors and the *E. coli* BL21 (DE3) expression strain (New England Biolabs).

Unlabeled proteins expressed by growing a culture in 10 mL LB per liter large culture, supplemented with 50 µg/mL kanamycin and 100 µg/mL spectinomycin (ACP), or 100 µg/mL streptomycin-sulfate (BmaI1), or 100 µg/mL Carbenicillin (EsaI) or 50 µg/mL kanamycin (Sfp, ACP_b) or 100 µg/mL kanamycin (ACPH) in a shaking incubator at 37 °C overnight.[7-10] The following morning, 1 L LB supplemented with appropriate antibiotics was inoculated with 10 mL of the overnight culture. The culture was grown in a shaking incubator at 37 °C until an OD_{600} of ~ 0.4, after which the temperature was reduced to 20 °C. At an OD_{600} of 0.7-0.9,

IPTG was added to a final concentration of 1 mM (ACP) or 0.5 mM (Sfp, ACPH, EsaI and BmaI1) and the proteins were expressed at 20 °C overnight. The next day, the bacteria were harvested by centrifugation at 6,000 x g for 15 min and the cell pellets were either stored at -80 °C or immediately prepared for purification.

Modified M9 minimal media for expression of U-$^{15}N^{13}C$ labeled ACP was prepared as follows: 6 g Na_2HPO_4, 3 g KH_2PO_4 and 0.5 g NaCl were dissolved in 1 L of double deionized water and autoclaved. Then, the appropriate antibiotic was added, as well as sterile filtered solutions of $MgSO_4$ (final concentration = 2.5 mM), $CaCl_2$ (final concentration = 0.1 mM), 2 g D-Glucose-$^{13}C_6$, 1 g $^{15}NH_4Cl$, 100 µL of a 10,000 x vitamin mix (5 g riboflavin, 5 g niacinamide, 5 g pyridoxine monohydrate and 5 g thiamine dissolved in ethanol), 50 mg U-^{15}N L-methionine and β -alanine at a final concentration of 8 µM. For the expression of U-^{15}N labeled proteins, 4 g D-Glucose was used in an otherwise identical medium. Cultures were grown from 10 mL LB overnight cultures in the same way described for unlabeled proteins.
Differently modified M9 minimal media for expression of U-$^{15}N^{2}H$ labeled ACP was prepared as follows: 6 g Na_2HPO_4, 3 g KH_2PO_4 and 0.5 g NaCl were dissolved in 1 L of D_2O in a dry autoclaved 2 L glass beaker. Then, 50 mg kanamycin and 100 mg spectinomycin were added, as well as sterile filtered solutions of $MgSO_4$ (final concentration = 2.5 mM), $CaCl_2$ (final concentration = 0.1 mM) in D_2O, 2 g D-Glucose-(1,2,3,4,5,6,6-d7), 1 g $^{15}NH_4Cl$, 100 µL of a 10,000 x vitamin mix (5 g riboflavin, 5 g niacinamide, 5 g pyridoxine monohydrate and 5 g thiamine dissolved in ethanol), 50 mg U-^{15}N L-methionine and β-alanine at a final concentration of 8 µM. The prepared medium was sterile filtered using a 0.2 µm filter.

25 mL LB media in D_2O per liter large culture were prepared by dissolving 0.625 g LB powder in 25 mL D_2O, supplemented with 50 μg/mL kanamycin and 100 μg/mL spectinomycin. The medium was sterile filtered using a 0.2 μm filter and inoculated with *E. coli* K-12 strain DK574 bearing the pJT94 plasmid and incubated in a shaking incubator at 37 °C for 10 h. The culture was centrifuged at 4,300 x g for 15 min and the bacterial cell pellet was gently resuspended in 50 mL of the modified M9 media in D_2O described above. This culture was grown in an Erlenmeyer flask at 37 °C overnight. The next morning, 1 L of the modified M9 media in D_2O described above was inoculated with 10 mL of the overnight culture. The bacteria were grown in a shaking incubator at 37 °C to an OD_{600} of ~ 0.4, after which the temperature was dropped to 20 °C. At this point, 1 g of Celtone Base Powder (D, 97 %+; ^{15}N, 98 %+, Cambridge Isotope Laboratories, Inc.) was added to the culture. Protein expression was induced at an OD_{600} of 0.7-0.9 with isopropyl β-D-1-thiogalactopyranoside (IPTG) at a final concentration of 1 mM. The next day, the bacteria were harvested by centrifugation at 6,000 x g for 15 min and the cell pellets were either stored at -80 °C or immediately prepared for purification.

U-^{15}N and U-$^{15}N^{13}C$-labeled ACP from *B. mallei* was expressed using a pHis-ACP_b (ATUM) construct transformed into *E. coli* BL21(DE3) expression strain. Isolated colonies from a kanamycin resistant plate were used to inoculate 5 mL Luria–Bertani broth supplemented with 50 μg/mL kanamycin (LB/Kan) and grown for 16 hrs at 37 °C, with shaking (220 rpm). The bacteria were pelleted at 4000×g for 5 min, the media decanted, and resuspended in 5 mL of M9 minimal media containing 50 μg/mL kanamycin with 2 g/L ^{13}C-glucose, and/or 0.5 g/L ^{15}N-NH_4Cl and 0.5 g/L ^{13}C and/or ^{15}N Isogro for isotope enrichment. These suspensions were used to inoculate 495 mL of M9/Kan with the appropriate isotopes. The cultures were grown at 37°C shaking at 220

rpm to an OD_{600} = 0.6 – 0.8 (~5 hrs). ACPb expression was induced with 0.5 mM IPTG at 30 °C for 16 hrs. The bacteria were pelleted at 4000×g for 15 min at 4 °C.

Purification of *E. coli* ACP (ACP_e).

Cell pellets were resuspended in ~ 30 mL resuspension buffer (50 mM Tris-HCl, pH = 7.5, 350 mM NaCl, 2 mM β-mercaptoethanol [BME], 1 mM ethylenediaminetetraacetic acid [EDTA], 1 cOmplete™ Protease Inhibitor Cocktail tablet [Sigma Aldrich]) per liter culture. Resuspended cells were then lysed by sonication (30 % amplitude, 5 min sonication time, 2 s on pulse, 4 s off pulse). Cell lysates were pelleted by centrifugation at 20,000g for 30 min at 4 °C. To transform holo-ACP into apo-ACP, cleared lysates were then incubated with 25 mM $MgCl_2$ and 1.2 mM $MnSO_4$ at 37 °C for 4 h. After this incubation period, protein was precipitated by addition of isopropanol to the cleared lysates to a final concentration of 50 % (vol/vol). Precipitated protein was pelleted using centrifugation at 20,000g for 30 min at 4 °C, and the supernatant was loaded onto diethylaminoethyl (DEAE)–Sepharose beads (Sigma Aldrich, ~ 5 mL per liter culture), preequilibrated with equilibration buffer (10 mM MES, pH = 6.1). Protein was incubated with resin at 4 °C for 16 h. The resin was washed with wash buffer (10 mM MES, pH = 6.1, 25 mM LiCl) until 10 µL of eluent no longer stained blue with 50 µL of Bradford reagent (Coomassie blue G-250, Bio-Rad). Bound protein was eluted with elution buffer (10 mM MES, pH = 6.1, 500 mM LiCl). The eluted protein was concentrated to a final volume of ~ 5 mL and subjected to size exclusion chromatography using a Superdex 75 increase 10/300 GL column preequilibrated with ACP buffer (50 mM MES, pH = 6.8, 10 mM $MgCl_2$, 1 mM TCEP-HCl).

Purification of *B. mallei* ACP (ACP_b).

Bacterial cell pellets were resuspended in 30 mL of the lysis buffer, B-PER complete (Thermofisher, Waltham, MA). The cells were incubated at RT for 30 min, and the protein containing supernatant was clarified by centrifugation at 20,000g for 45 min at 4 °C. The supernatant was filtered through a 0.45 μm polyethersulfone (PES) filter and loaded onto a 1 ml Ni–NTA HisTrap (Cytiva, Marlborough, MA) that had been pre-equilibrated with 20 mM Tris HCl pH 7.9, 250 mM NaCl, 20 mM imidazole, 10% (v/v) glycerol (Wash Buffer). After sample loading, the column was washed with 5 column volumes of the wash buffer. Tagged proteins were eluted, using a buffer containing 200 mM imidazole (Elution Buffer). Fractions containing purified protein were identified using 16% tris-tricine-PAGE, pooled, buffer exchanged into storage buffer (137 mM NaCl, 2.7 mM KCl, 8 mM Na_2HPO_4, 2 mM KH_2PO_4, 0.1 mM EDTA, 0.1 mM TCEP, 0.02 mM NaN_3, and 25% glycerol) and concentrated using Vivaspin 3000 MWCO centrifugal filter devices. Aliquots were flash frozen in liquid nitrogen and stored at -80 °C. The protein was purified as holo:apo mixture. Prior to NMR experiments, isotopically labeled apo-ACPb was further purified using size-exclusion chromatography (HiLoad 16/600 Superdex 75 pg) on an ÄKTA pure 25 FPLC (Thermofisher, Waltham, MA) equilibrated with 50 mM 2-ethanesulfonic acid, pH 6.8, 10 mM magnesium chloride, 1 mM tris(2-carboxyethyl)phosphine) and concentrated using Vivaspin 3000 MWCO centrifugal filter devices.

Purification of *P. aeruginosa* ACPH.

Bacterial cell pellets were thawed on ice for 20-30 minutes followed by the addition of 3 mL of B-PER lysis reagent (Thermofisher, Waltham, MA) per gram of the pellet. DNAse and RNAse (20 μL/gram of cell pellet, 5 mg/mL stock), lysozyme (40 μL/gram of cell pellet, 40 mg/mL stock)

and Phenylmethylsulfonylfluoride (60 µL/gram of cell pellet, 13 mg dissolved in 750 µL isopropyl alcohol) were added to this cell suspension. The lysate mixture was incubated at room temperature for 10-20 minutes and centrifuged at 20,000g for 45 minutes. The protein-containing supernatant was loaded on to Ni-NTA column (BioRad, Hercules, CA) pre-equilibrated with 50 mM Tris-HCl, 0.5 M NaCl, pH 7.5 buffer (Equilibration Buffer). The column was washed with 12 column volumes of equilibration buffer containing 20 mM imidazole (Wash Buffer) and 8 column volumes of equilibration buffer containing 300 mM imidazole (Elution Buffer). Pooled fractions were filtered using a 0.45 µm polyethersulfone (PES) filter and subjected to size exclusion chromatography using an isocratic 50 mM sodium phosphate, 100 mM NaCl, pH 6.0 buffer (Enrich SEC650, BioRad). The cleaned ACPH fractions were desalted and buffer-exchanged using a PD-10 column (Cytiva, Marlborough, MA). Glycerol was added to store the protein fractions in 20% glycerol. Protein aliquots were flash frozen and stored at -80 ^{o}C until further use.

Purification of *B. subtilis* Sfp, *B. mallei* BmaI1 and *P. stewartii* EsaI.

Bacterial cell pellets were resuspended in ~ 15 mL resuspension buffer (50 mM Tris-HCl, pH = 8.0, 350 mM NaCl, 10 mM imidazole, 2 mM β-mercaptoethanole [BME], 1 cOmplete™ Protease Inhibitor Cocktail tablet [and 5 % glycerol for BmaI1) per liter culture. Resuspended cells were then lysed by sonication (30 % amplitude, 5 min sonication time, 2 s on pulse, 4 s off pulse). Cell lysates were pelleted by centrifugation at 30,000g for 40 min at 4 °C. Cleared lysates were incubated with ~ 3 mL Ni-NTA agarose resin (Thermo Fisher), preequilibrated with wash buffer (50 mM Tris-HCl, pH = 8.0, 350 mM NaCl, 10 mM imidazole, 2 mM BME [and 5 % glycerol for BmaI1) per liter culture for 2-16 h at 4 °C. The resin was washed with wash buffer until 10 µL of eluent no longer stained blue with 50 µL of Bradford reagent (Coomassie blue G-250). Bound

protein was eluted with elution buffer (50 mM Tris-HCl, pH = 8.0, 350 mM NaCl, 350 mM imidazole, 2 mM BME). Eluted protein was concentrated to ~ 15 mL and subjected to size exclusion chromatography using a Superdex 75 increase 10/300 GL (Cytiva) column preequilibrated with SEC buffer (50 mM MES, pH = 6.8, 100 mM NaCl, 10 mM $MgCl_2$, 1 mM TCEP-HCl).

Conversion of holo-ACP_b to apo-ACP_b.

The holo-ACP percent in the holo:apo mixture was calculated using peak areas in the HPLC chromatogram. A solution of 200 µM holo-ACP (based on % holo-ACP) was incubated with 5 µM ACPH in 50 mM Tris-HCl buffer (pH 8) in 15 mM $MgCl_2$, 1 mM $MnCl_2$, and 100 mM NaCl. Conversion of the residual holo-ACPb to apo-ACPb was monitored through HPLC chromatogram.

General procedure for Alkyl-ACP synthesis.

For alkyl-ACP synthesis, apo-ACP was concentrated to concentrations between 100-500 µM in ACP NMR buffer (50 mM MES, pH = 6.8, 10 mM $MgCl_2$, 1 mM TCEP-HCl) and combined with 1 µM purified Sfp and 1.25 equivalents (with respect to apo-ACP) of either 3-oxoC6iCoA, 3-oxoC8iCoA, C6iCoA or C8iCoA. The reaction mixture was allowed to incubate at 25 °C for 1 h and reaction completion was confirmed by ^{15}N-^{1}H-HSQC NMR spectra.

NMR experiments.

Triple resonance backbone experiments were recorded on a Bruker Avance III 800 MHz spectrometer with a TXO-style cryogenically cooled probe, operating at 800 MHz proton frequency at 310 K. ACP isoforms were concentrated to 500 µM in ACP NMR buffer (50 mM MES, pH = 6.8, 10 mM $MgCl_2$, 1 mM TCEP-HCl). For backbone resonance assignment, HNCA, HN(CO)CA, HNCACB, HNCO, HN(CA)CO and CCCONH experiments were recorded. All 3D

spectra were acquired using non-uniform sampling (NUS) with 10% sampling of the Nyquist grid using Poisson Gap Sampling.[11] The NUS spectra were reconstructed and processed with hmsIST.[12] For titration experiments, apo-ACP, 3-oxoC6iACP, 3-oxoC8iACP, C6iACP and C8iACP were concentrated to a final concentration of 100 µM. Standard HSQC experiments with sensitivity enhancement from the Bruker library were recorded for ^{15}N-labeled ACP isoforms at 310 K on a Bruker Avance III 800 MHz spectrometer with a TXO-style cryogenically cooled probe, operating at 800 MHz proton frequency. A typical HSQC experiment was recorded with 256 increments in the indirect dimension with 16 scans, leading to an experimental time of approximately 40 minutes. Unlabeled EsaI and BmaI1 samples were titrated, and HSQC experiments were recorded. Chemical shift perturbations (CSPs) were calculated using the formula

$$CSP = (\Delta \delta H^2 + [0.14 \Delta \delta N]^2)^{1/2},$$

where $\Delta \delta H$ and $\Delta \delta N$ are the changes in chemical shifts for proton and nitrogen frequencies, respectively, in ppm. Signal intensity reduction was calculated using the formula

Intensity reduction [%] = Peak height (in presence of ligand) / Peak height (in absence of ligand) * 100 %

NMR experiments were processed with NMRPipe[22] and analyzed using the ccpNMR software (version 2.4.1).[23]

Based on calculated CSPs, proteins were colored using "B-factors" in pymol[20]. Here, the numerical CSP values were entered into a text file and assigned as B-factors and the protein was colored using a blue_white_red gradient with the average CSP set as minimum and the highest value set as maximum.

Cross saturation transfer (CST) NMR measurements, which exclusively provides information on the direct interaction interface[24, 25, 26]. The experiments were recorded using 50 µM ^{2}H-^{15}N-

labelled 3-oxo-C6i ACP and 100 μM unlabeled EsaI in a buffer with 70% $^{2}H_2O$-content. Experiments were measured with on (0 ppm) and off-resonance saturation (−30 ppm) in an interleaved fashion using 50 μM 3-oxo-C6 ACP in ACP NMR buffer. The samples were prepared in 70% v/v $^{2}H_2O$ to minimize spin-diffusion through solvent. Saturation time was set to 3 s and recycle delays to 1 s. Composite WURST pulses (25 milliseconds in duration) were used for saturation. 200 increments in the indirect dimension were recorded with 128 scans, leading to an experimental time of approximately 30 hours. The CST plot was created by plotting the ratio between signal intensities off resonance and signal intensities on resonance.

Deposition of NMR assignments: The NMR resonance assignment has been deposited in the BRMB database and can be accessed with the code 51560 (apo-ACPp from Escherichia coli), 51561 (3-oxo-C6i ACPp from Escherichia coli), 51562 (HN resonances of C8i ACPp from Escherichia coli, assignment assisted by BMRB 50756 deposition), 51563 (HN resonances of C6i ACPp from Escherichia coli) and 51564 (HN resonances of 3-oxo-C8i ACPp from Escherichia coli)

Docking Method.

The BmaI structure used in the study was constructed through homology modeling in the SwissModel Homology modeling webserver[15] with the TofI structure 3P2H from *Burkholderia glumae*. The *Pantoea stewartii* AHL-synthase EsaI was modeled from the 1KZF crystal structure. Before docking, all the AHL-synthase models were solvated using the ICM quickflood procedure.[16] After solvation, the AHL-synthases were minimized using the ICM optimizeHbonds and optimizeHisProAsnGlnCys protocols. Solvation and minimization have previously been found to be necessary for accurate prediction of docked complexes.[17] The EsaI T140A mutant was constructed using the Mutate utility in ICM.[18] The mutated protein was solvated and minimized

identically to the wild-type protein. apo-ACP was derived in a similar manner to the partner proteins, where the PDB structure 2K92 was solvated and minimized to prepare it for docking. ACPs used for docking were derived from previously run MD simulations. In the case of C8, C6, and C8-oxo the structures were taken directly from previously published simulations.[19] The 3-oxoC6ACP was constructed by first manually modifying the PDB in the Pymol Builder utility.[20] Next, the ACP was minimized in the region surrounding helix III to allow for the readjustment of the ACP to the new cargo. The results were verified against the MD derived models to ensure that the method made an accurate prediction of the C6-oxo structure.

Docking of all ACPs and the partner proteins was performed in the ICM – Molsoft FFT protein-protein docking algorithm.[21] Focus residues were given based on the experimentally derived CSPs, while the conformation of the acyl chain and 4'-phosphopantetheine were kept frozen during the docking. Docked models were evaluated based on the total energy prediction from the ICM algorithm.[18, 21] The energy values do not directly translate to binding potentials, but are accurate enough for internal comparison. In the cases of improper substrates, such as the apo-AcpP, the conformation which was within interacting distance with the active site was chosen. Lower energy states where the apo-AcpP interacted far from the active site were ignored. Analysis was also performed by viewing the structures in PyMol and all visualizations were rendered in PyMOL.[20]

Intact mass spectrometry analysis of cargo-labeled ACP proteins.

^{15}N-Cargo-labeled ACP proteins in buffer (MES pH 6.8, 10 mM MgCl2, 1mM TCEP) were diluted to 50 ng/µL in 50 mM ammonium bicarbonate (pH 8.0) and centrifuged at 15,000 x g for 5 min. We used ^{15}N-labeled proteins to ensure we can observe and validate the cargo-induced NMR chemical shifts on the same protein that we perform the mass spectrometry. Supernatants were

transferred to liquid chromatography vials, and approximately 25 ng of each protein sample was loaded onto a Vanquish Flex LC linked to a Q Exactive mass spectrometer (Thermo Fisher). Proteins were separated by reversed liquid phase chromatography on an MAbPac RP 3 µm 2.1 x 100 mm column (Thermo Fisher #088647) at a flow rate of 0.3 mL/min with a 2 min isocratic hold at 5% mobile phase B (0.1% (v/v) formic acid in acetonitrile), followed by a linear gradient from 5-80% mobile phase B over 16 min, where mobile phase A was 0.1% (v/v) formic acid in water. Mass analysis with the Q Exactive (Tune version 2.1) was performed in Full MS mode. Four microscans per duty cycle were obtained with a resolution of 70,000 and an m/z scan range of 500-1600. The AGC target was set to 3,000,000 with a maximum ion injection time of 200 ms. For each cargo-labeled ACP protein, MS scans were averaged across the corresponding chromatographic peak, and the resulting spectra were deconvoluted using UniDec software.

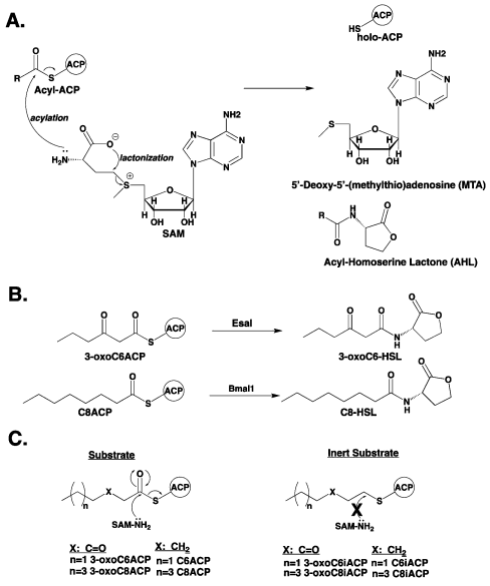

Figure S1A. Substrates and products of AHL synthesis. A. Mechanism of AHL synthesis. B. Acyl-substrate and AHL products of EsaI and BmaI1-catalyzed AHL synthesis. C. Alkyl-ACP inert substrates used in this study.

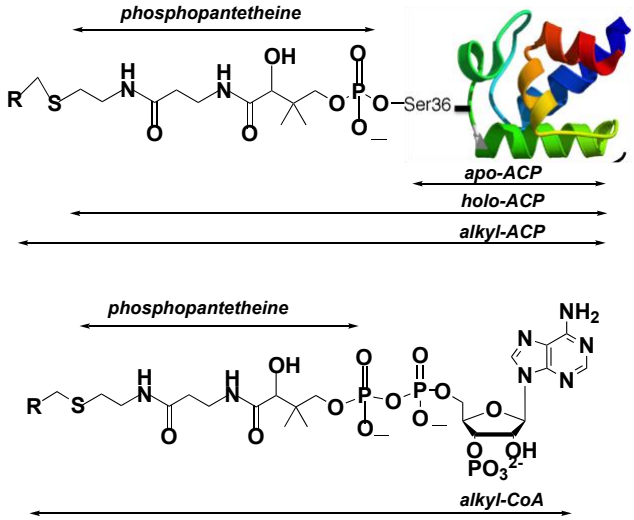

Figure S1B. Structural differences between alkyl-ACP and alkyl-CoA.

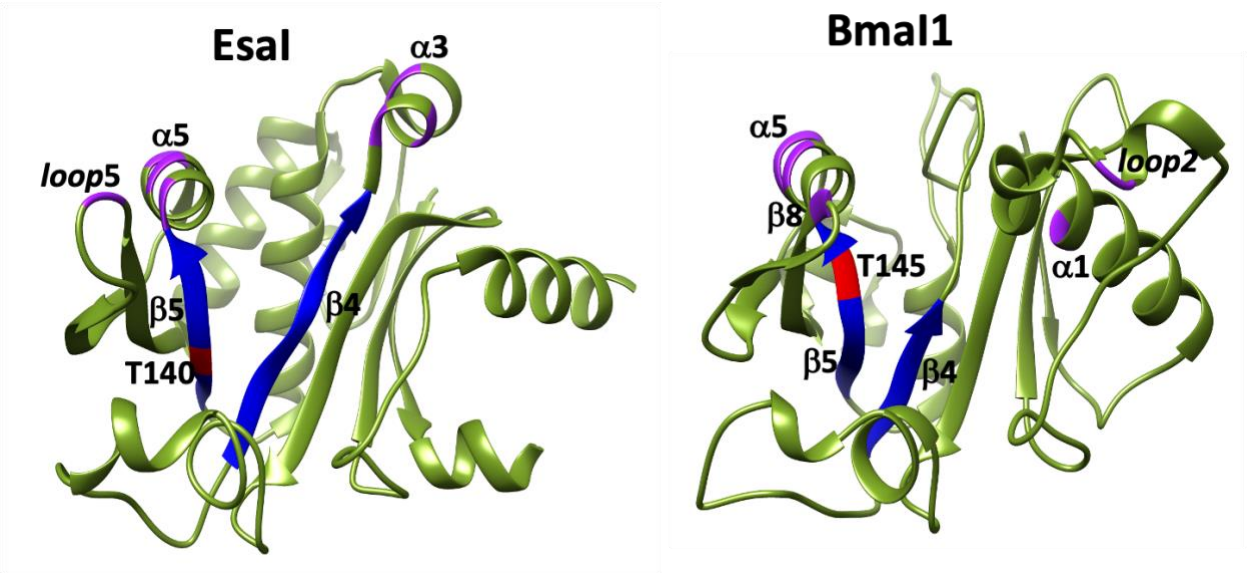

Figure S2. EsaI and BmaI1 structures.
The V-shaped cleft that accommodates the acyl-chain cargo of the acyl-ACP substrate is highlighted in blue. The 3-oxoengaging threonines in both enzymes are highlighted in red. The basic patch of residues in the enzyme that forms electrostatic protein-protein contact with the carrier protein (ACP binding site) is highlighted in purple.

```
                          H1              L1                  H2        L2   H3
B.malleiACP          MDNIEQRVKKIVAEQL GVAEAEIKNEASFVNDLGADS LDTVELVMALEDEFG MEIPD EEA  60
E.coliACP            MSTIEERVKKIIGEQL GVKQEEVTNNASFVEDLGADS LDTVELVMALEEEFD TEIPD EEA  60
P.stewartiiACP       MSDIEQRVKKIISEQL GVKEEEVTNSASFVEDLGADS LDTVELVMALEEEFD TEIPD EEA  60
                     *. **:*****: *** ** : *:.*.****:****** ***********:**.  **** ***

                        L3        H4
B.malleiACP          E KITTV QQAIDYARANVKA       79
E.coliACP            E KITTV QAAIDYINGHQA-       78
P.stewartiiACP       E KITTV QAAIDYINSHKG-       78
                     * ***** * ***: ..:
```

Figure S3. Sequence alignment between *E. coli*, *B. mallei* and *P. stewartii* ACPs.
E. coli ACP shares 74% and 90% identities, respectively with *B. mallei* and *P. stewartii* carrier proteins. Note that the percent identities in helices II, III and loops 2 and 3 (the CSP producing regions) among the three ACPs are greater than 95%. H and L, respectively, refer to helix and loop in the carrier protein.

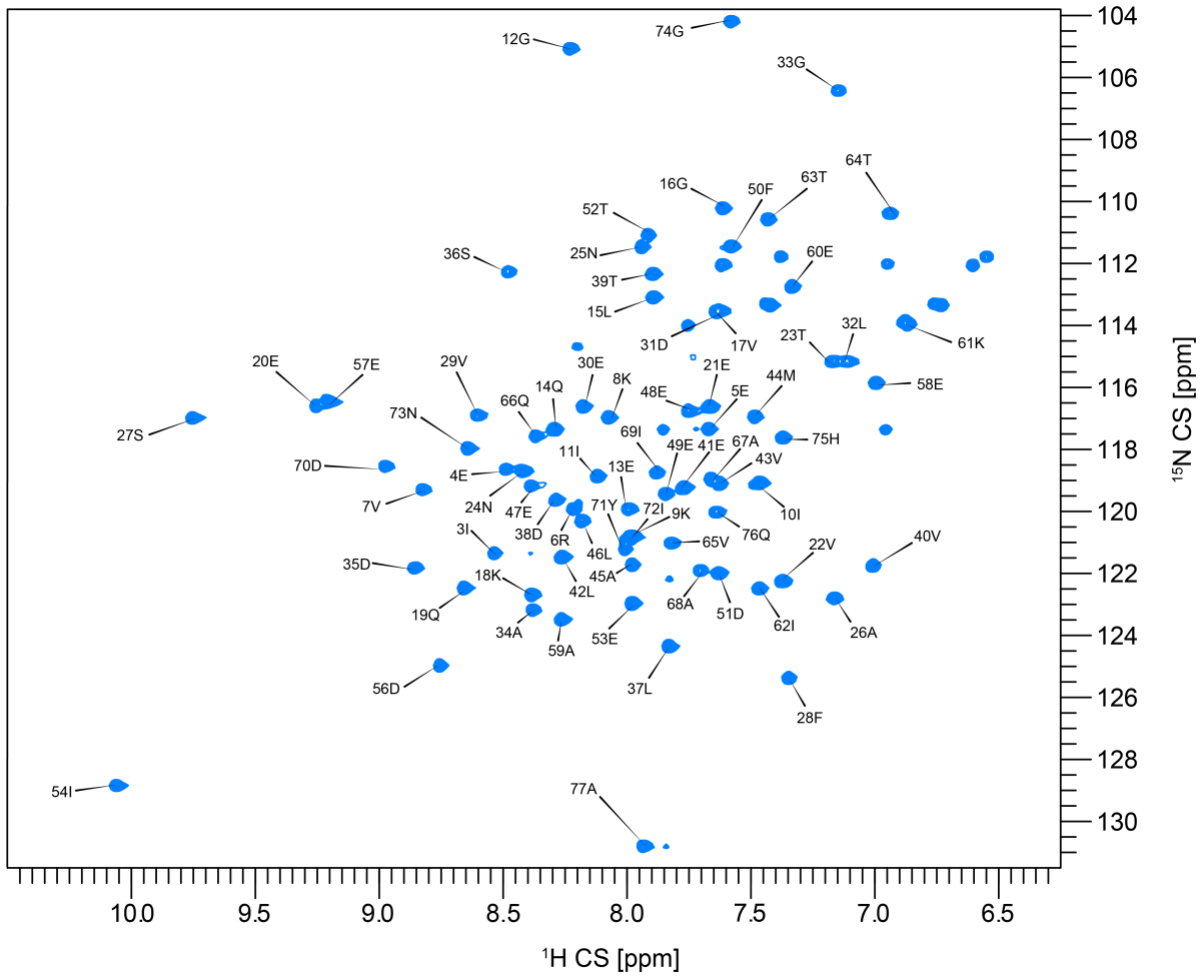

Figure S4. Backbone Resonance Assignment of 3-oxohexyl-ACP.

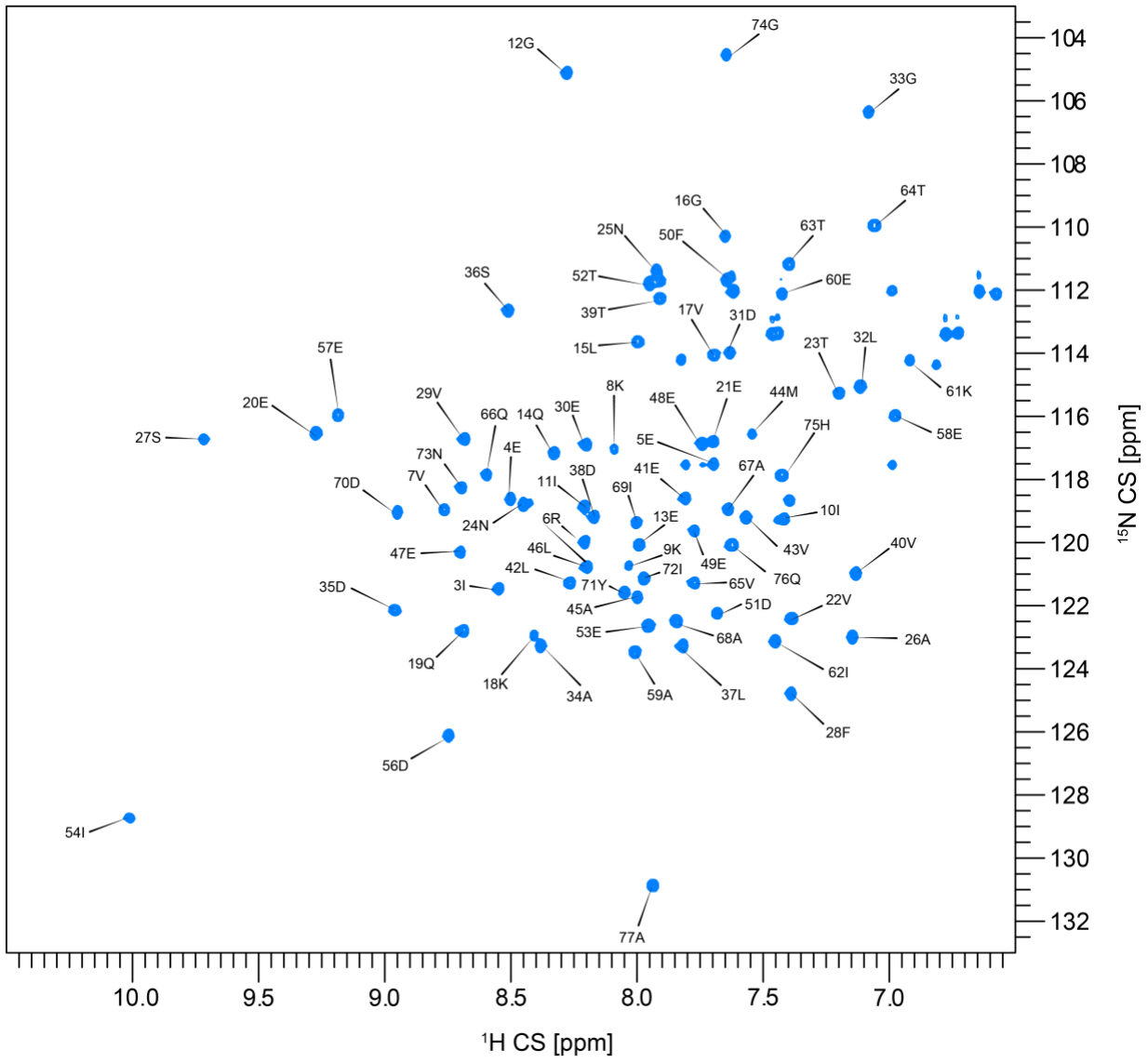

Figure S5. Backbone Resonance Assignment of octyl-ACP.

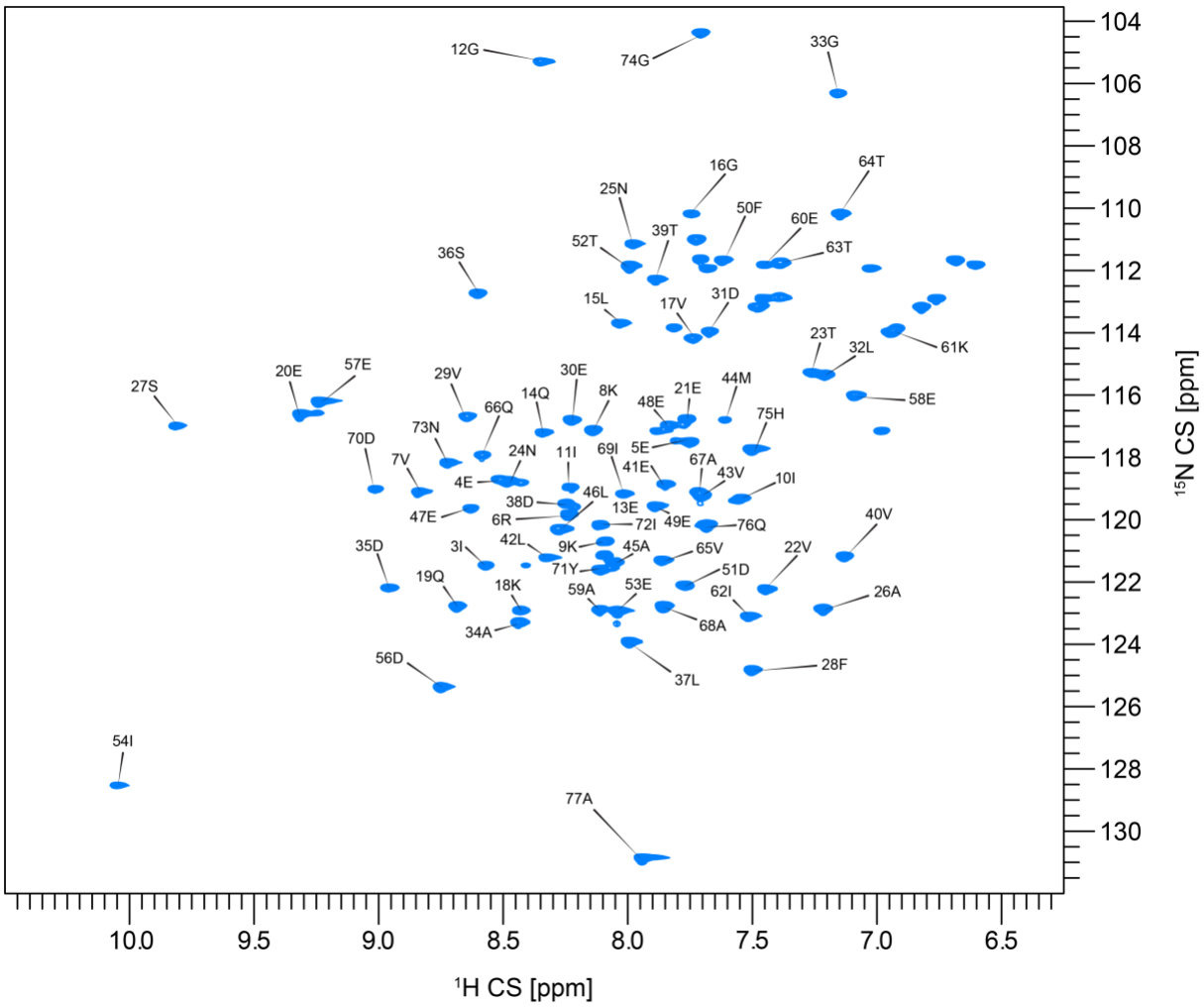

Figure S6. Backbone Resonance Assignment of 3-oxooctyl-ACP.

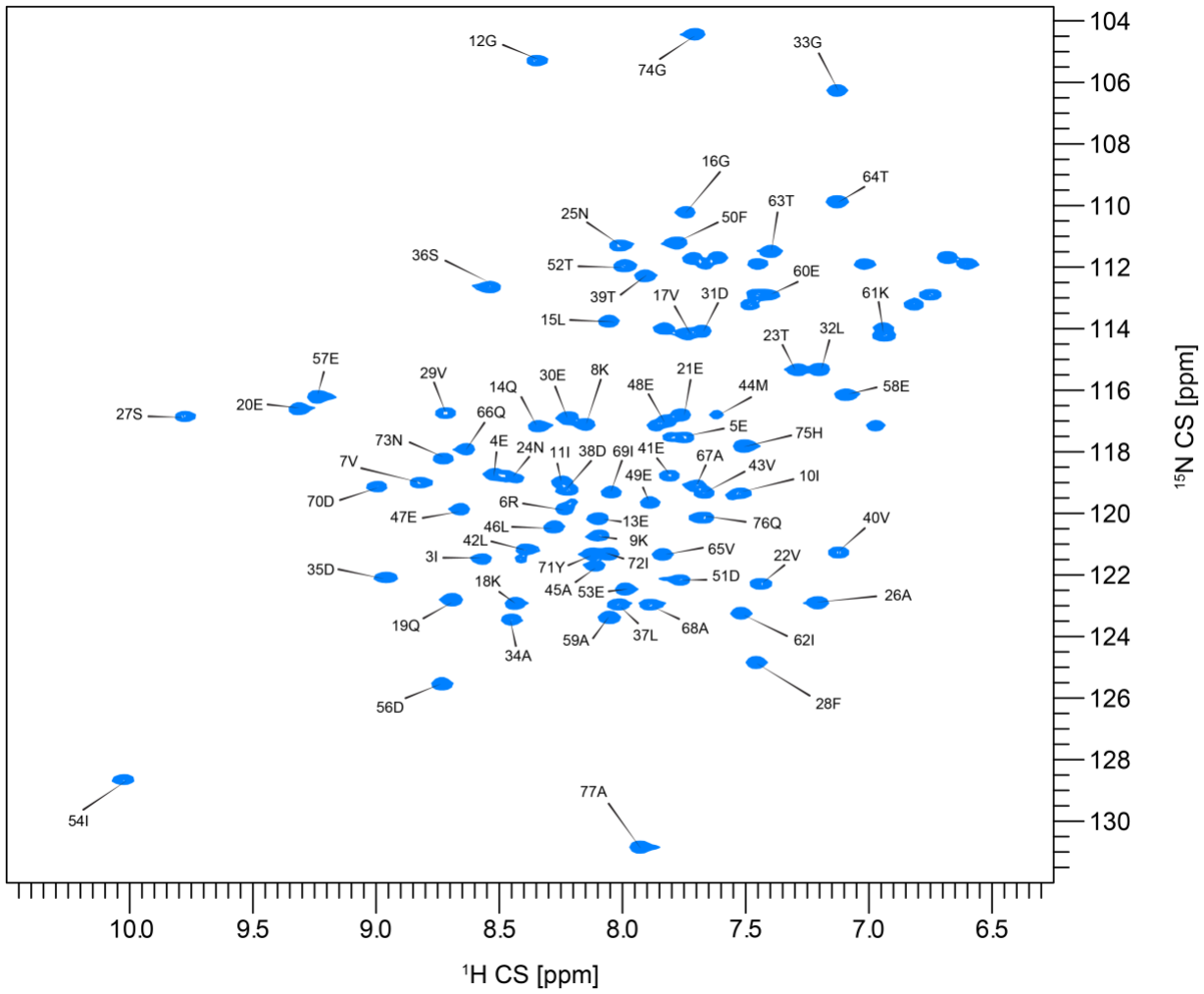

Figure S7. Backbone Resonance Assignment of hexyl-ACP.

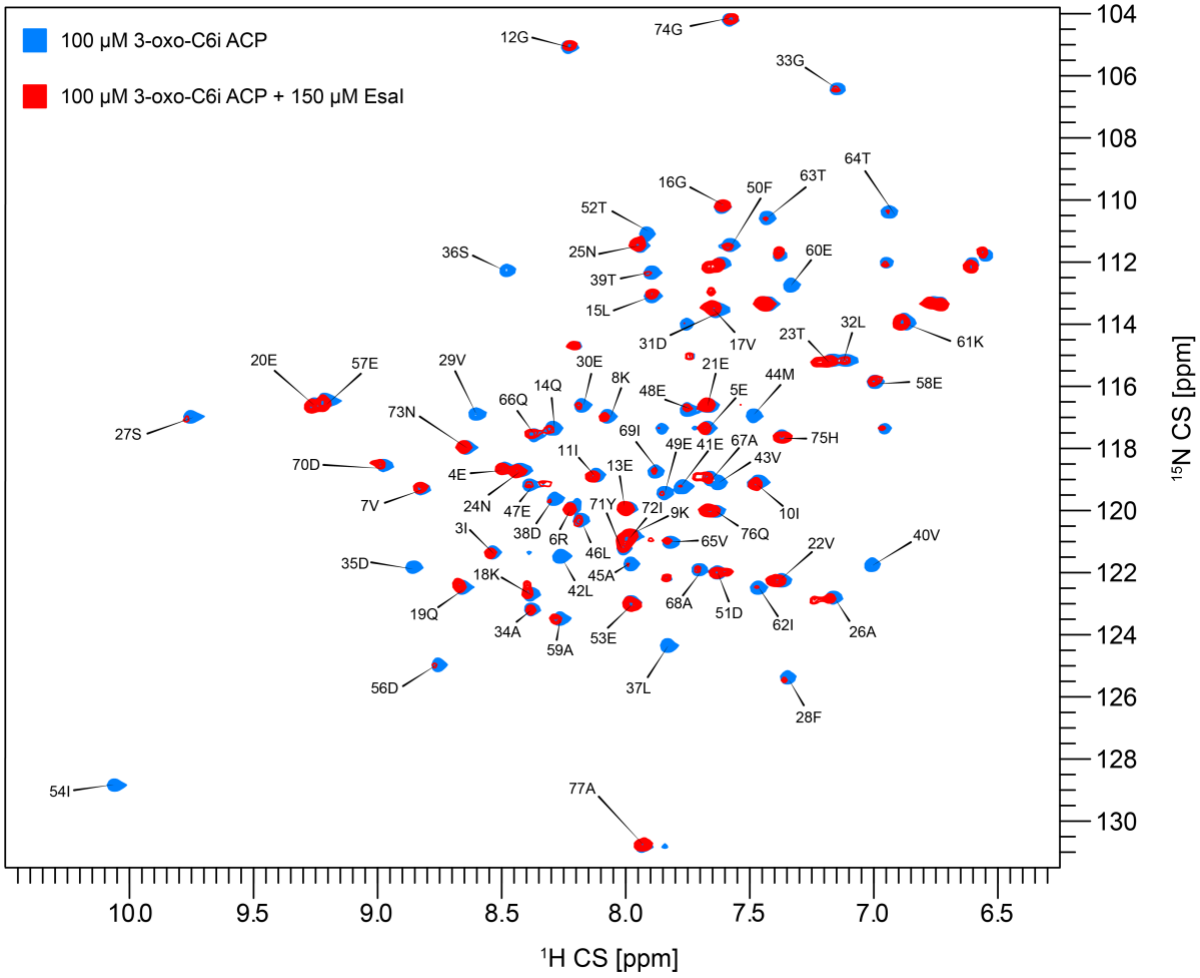

Figure S8. Chemical shift perturbation analysis of 3-oxohexyl-ACP bound to EsaI.

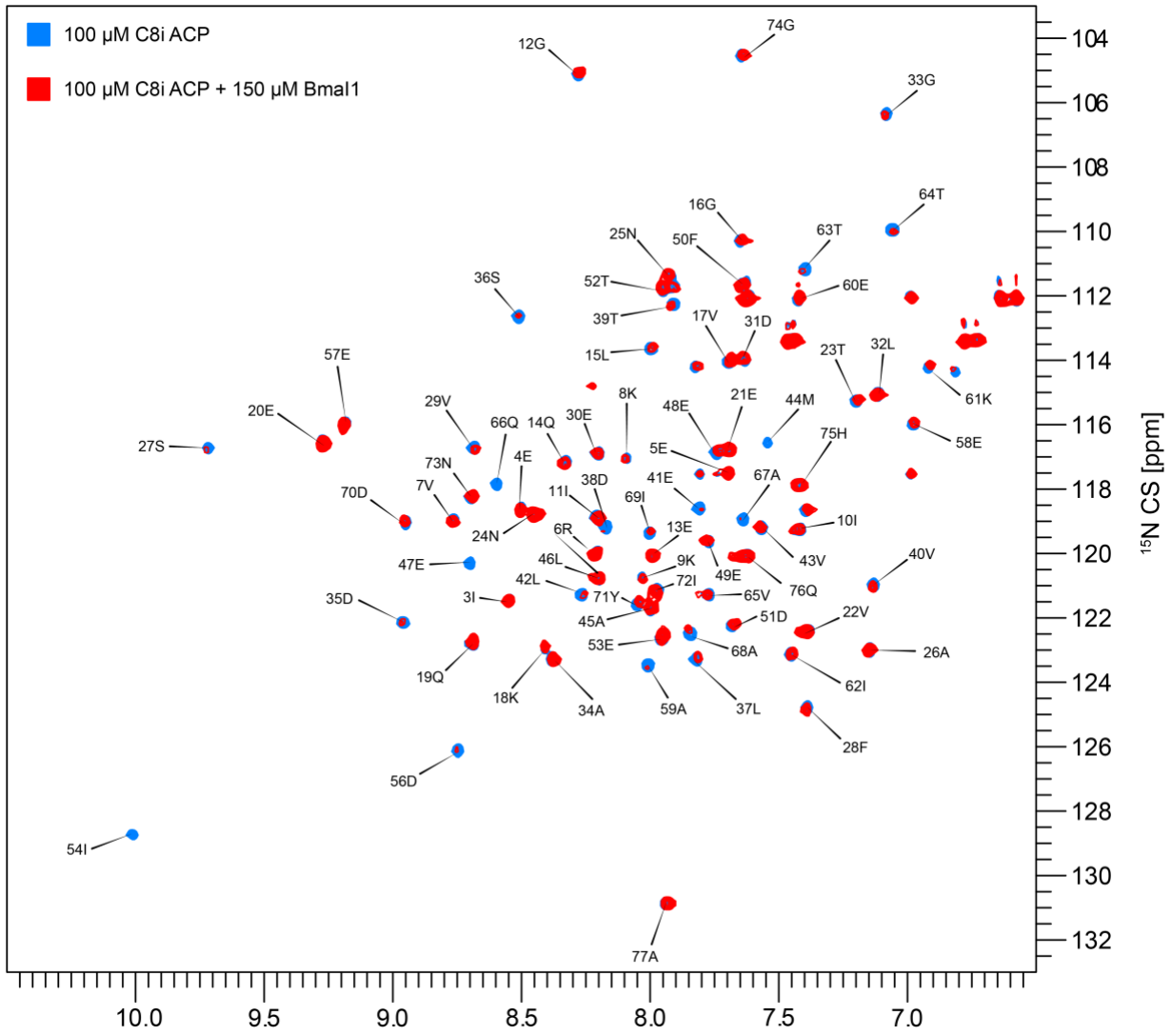

Figure S9. Chemical shift perturbation analysis of octyl-ACP bound to BmaI1.

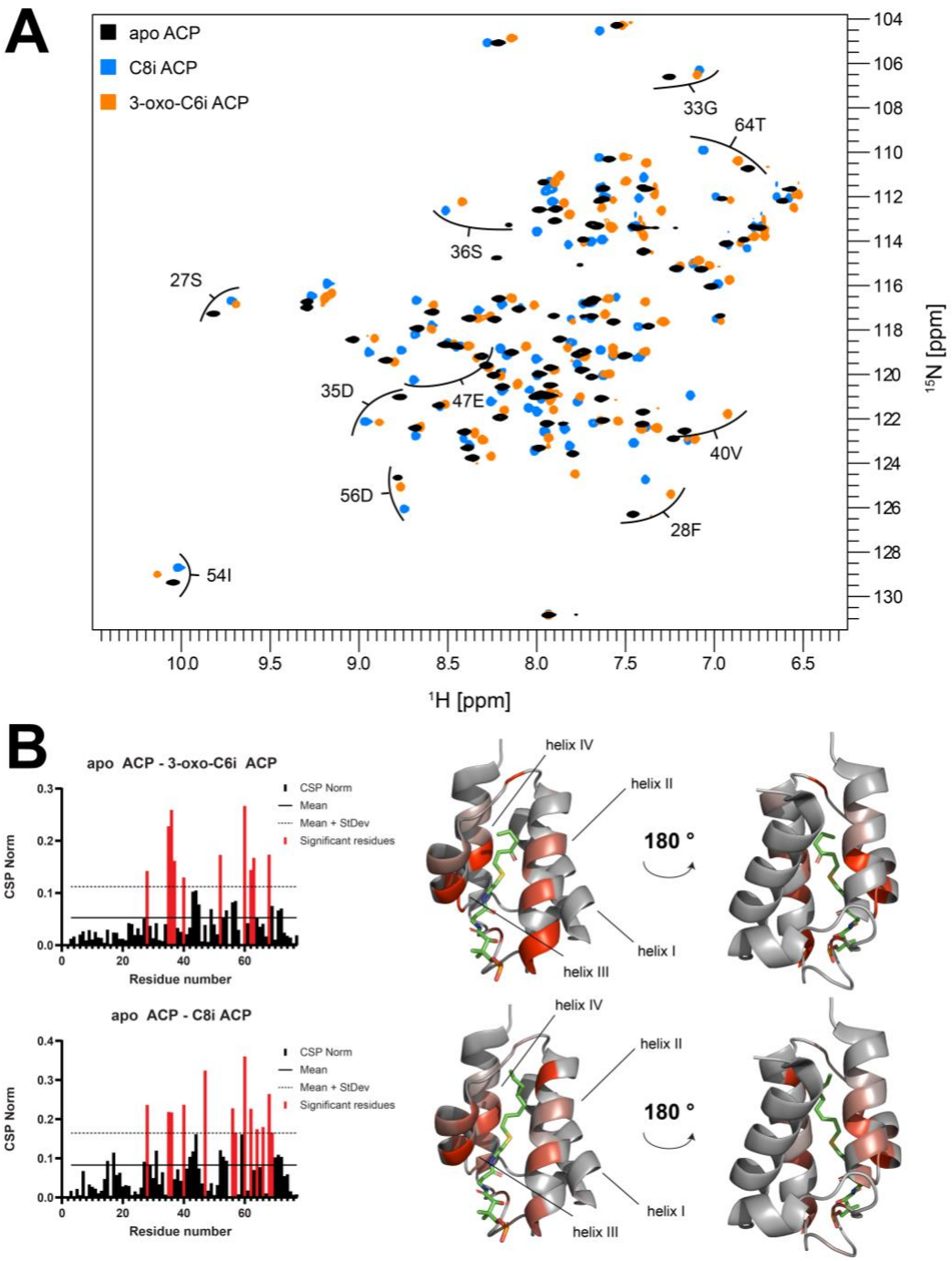

Figure S10. Chemical shift perturbation analysis of apo and cargo-loaded acyl carrier proteins.

A. ^{15}N-^{1}H-HSQC overlay of apo ACP (black), C8i ACP (blue) and 3-oxo-C6i ACP (orange). B. CSPs between apo ACP with 3-oxo-C6i ACP (top) and apo ACP with C8i ACP (bottom) as a function of residue number. Weighted CSPs are plotted on the structure of heptanoyl ACP (PDB ID 2FAD) with modified acyl chains. A color gradient is applied from average CSP (grey) to the highest observed CSP (red).

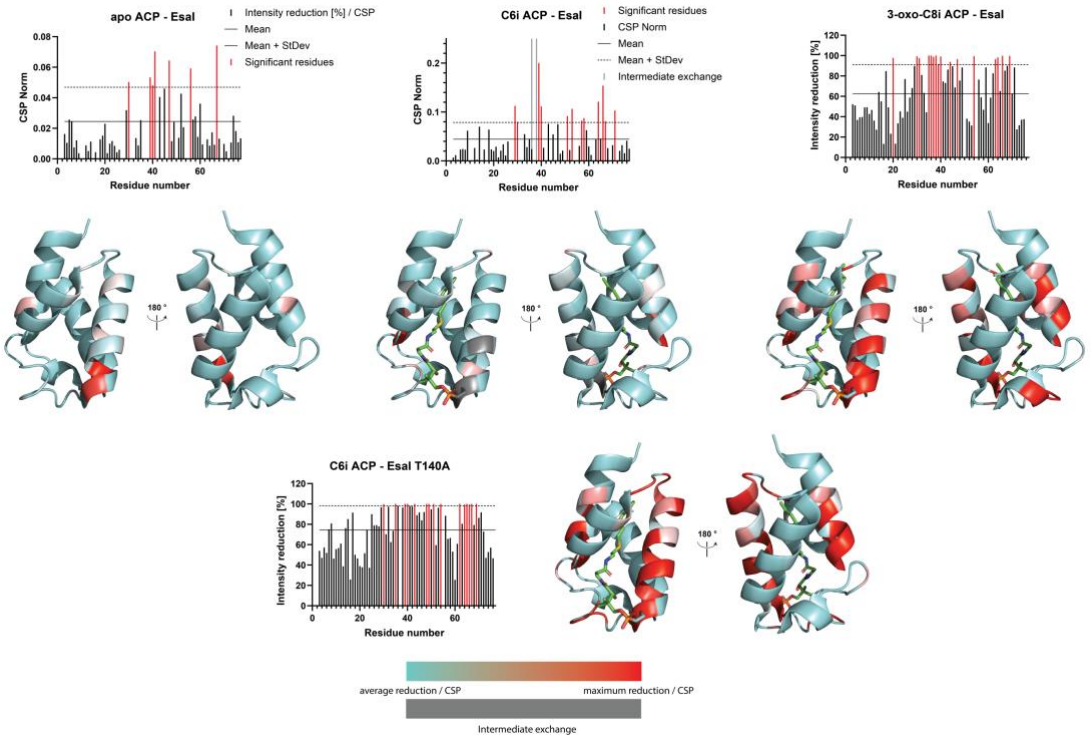

Figure S11. Chemical shift perturbation analysis of non-native cargo-loaded acyl carrier proteins bound to EsaI.

Top: Binding interfaces between apo ACP, C6i ACP and 3-oxo-C8i ACP with EsaI. Bottom: Binding interface between C6i ACP and EsaI T140A. Intensity reduction of peaks in ^{15}N-^{1}H-HSQC spectra of loaded ACPs after introduction of AHL synthase are plotted as a function of residue number. CSP data are plotted on the structure of heptanoyl ACP (PDB ID 2FAD) with modified acyl chains. A color gradient is applied from average reduction (cyan) to the highest observed reduction (dark red).

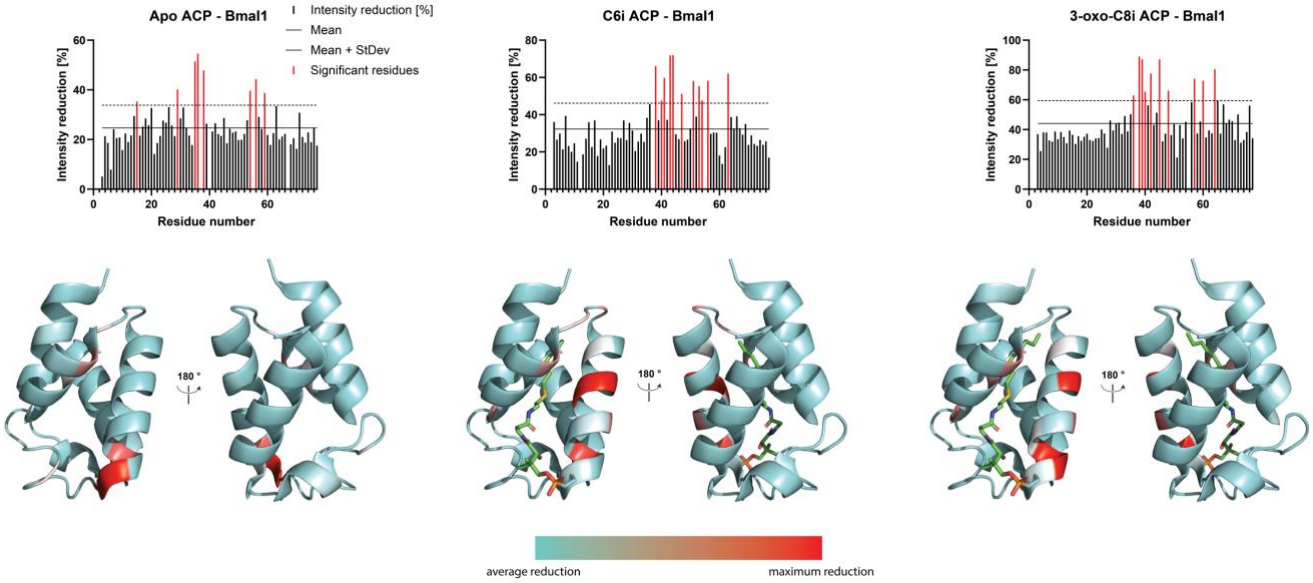

Figure S12. Chemical shift perturbation analysis of non-native cargo-loaded acyl carrier proteins bound to BmaI1.

Binding interfaces between apo ACP, C6i ACP and 3-oxo-C8iACP with BmaI1. Intensity reduction of peaks in ^{15}N-^{1}H-HSQC spectra of loaded ACPs after introduction of AHL synthase are plotted as a function of residue number. CSP data are plotted on the structure of heptanoyl ACP (PDB ID 2FAD) with modified acyl chains. A color gradient is applied from average reduction (cyan) to the highest observed reduction (dark red).

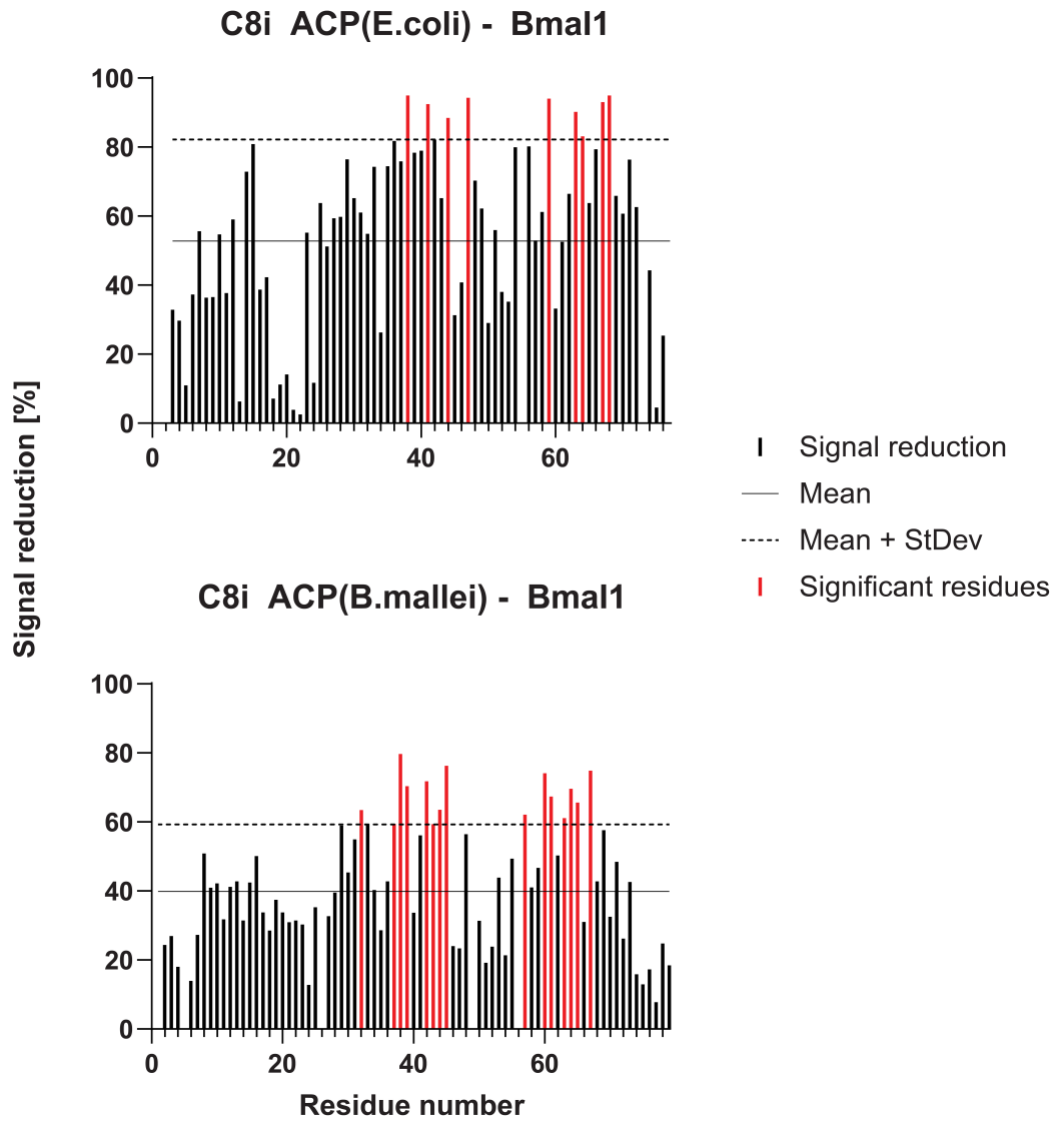

Figure S13. Chemical Shift Perturbation Analysis of octyl-ACP$_e$ vs octyl-ACP$_b$ titration with BmaI1.

The octyl (C8) cargo loaded carrier proteins from *E. coli* (top) and *B. mallei* (bottom) were titrated with BmaI1 AHL synthase. The CSPs in [BmaI1.C8iACP$_b$] were widespread similar to [BmaI1.C8iACP$_e$] ES complex. The enhancement in the specificity of BmaI1-ACP$_b$ interactions is evident from the increase in CSPs for this complex compared to BmaI-ACP$_e$ complex.

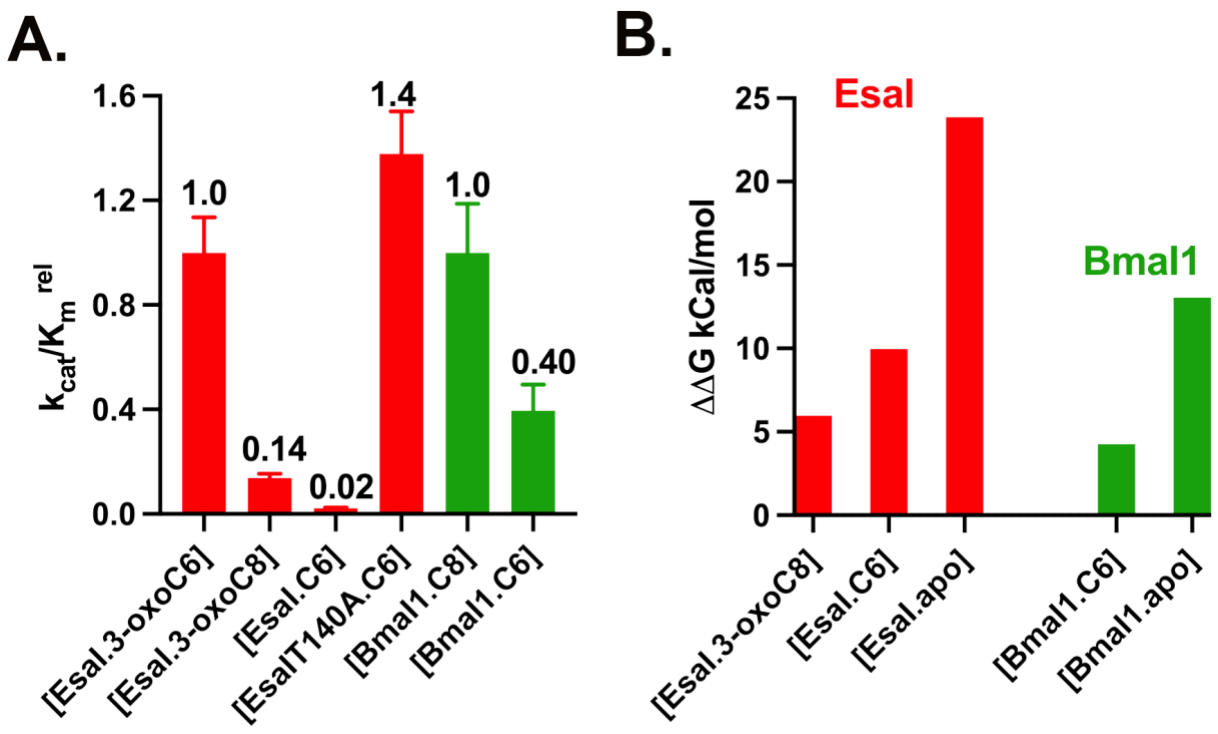

Figure S14. Native vs Nonnative ES complexes in EsaI and BmaI1.
A. Experimentally determined relative catalytic efficiencies in productive, lessproductive and nonproductive ES complexes. The k_{cat}/K_m^{rel} was calculated by dividing $k_{cat}/K_m^{nonnative}$ over k_{cat}/K_m^{native} substrates (EsaI: $k_{cat}/K_m^{rel} = k_{cat}/K_m$ / $k_{cat}/K_m^{3\text{-}oxoC6ACP}$; BmaI1: $k_{cat}/K_m^{rel} = k_{cat}/K_m$ / k_{cat}/K_m^{C8ACP}). The kinetic constants from Table S1 were used in these calculations. The native substrate for EsaI and BmaI1, respectively are furanacetyl-ACP (3-oxoC6-ACP mimic) and C8-ACP. The k_{cat}/K_m for T140A was calculated using the equation $k_{cat}/K_m^{rel} = k_{cat}/K_m^{EsaIT140A\text{-}C6ACP}$ / $k_{cat}/K_m^{EsaI\text{-}3\text{-}oxoC6ACP}$. The values above each bar represent the k_{cat}/K_m^{rel} in each enzyme-substrate pair. Lower k_{cat}/K_m^{rel} numbers reflect poorer substrate. B. Docking predicted free energy differences between native and nonnative ES complexes. ΔΔG values were calculated using the following equation: $\Delta\Delta G = \Delta G^{non\text{-}native[ES]} - \Delta G^{native[ES]}$. The native ES complex for EsaI and BmaI1, respectively are [EsaI.furanacetyl-ACP] and [BmaI1.C8-ACP]. Although the absolute values in free energies differed between computation and experiments, the relative trends in free energies determined from docking match the trends in catalytic efficiencies determined from experiments.

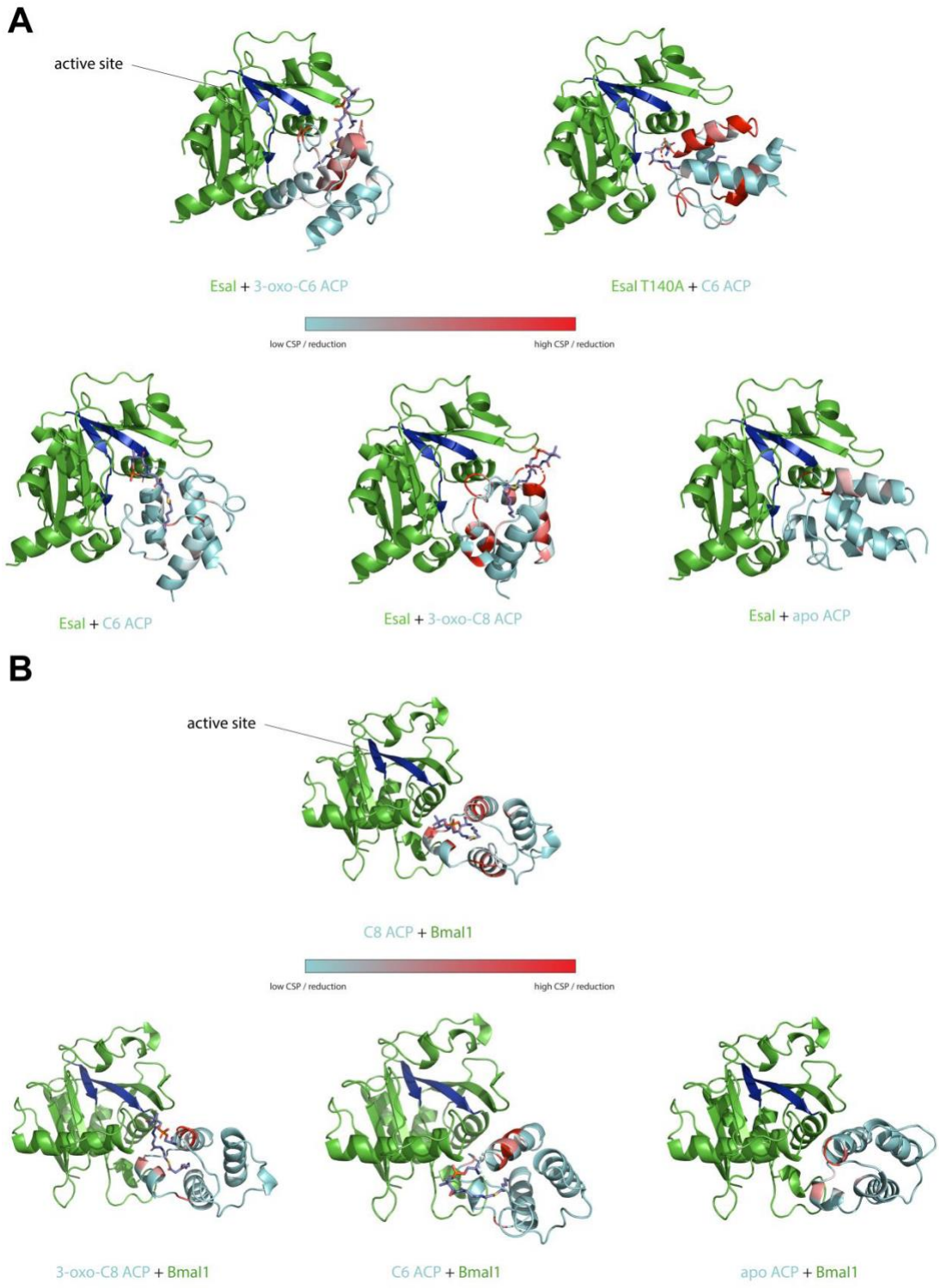

Figure S15. Docking poses of cargo-loaded acyl carrier proteins bound to EsaI and BmaI1. Docking analysis gives a visual representation of productive / less productive / nonproductive enzyme-substrate complexes. The acyl-chain pocket in EsaI and BmaI1 are highlighted in blue.

A) Binding interfaces of apo, native and non-native cargo-loaded ACPs to EsaI wild-type and T140A mutant. During initial docking, the acidic residues in the ACP (predominantly from helix II) binds to the basic patch in the helix V, loop 8 (connecting β6 and β7) and helix III of the EsaI enzyme. In the productive EsaI.3-oxoC6iACP] complex ACP loop 1 and helix II effectively engages the helix V and loop 8 basic cluster in the enzyme. In addition, the loop 1 in ACP interacts with the basic patch of residues in EsaI helix III. In the nonproductive [EsaI.C6iACP], the orientation of ACP is orthogonally aligned to the enzyme, thereby losing the entire set of productive interactions between the carrier protein and the enzyme. The binding pose of the less productive [EsaI.3-oxoC8iACP], however, is intermediary between the productive 3-oxoC6iACP and the nonproductive C6iACP poses with the enzyme. Due to the nonoptimal binding mode, it appears that the protein-protein contact in this ES complex has a larger footprint comprising ACP helix II – Enzyme loop 8, ACP loop 1 - Enzyme helix V and ACP helix III - Enzyme helix III interacting surfaces. Furthermore, ACP helices III and IV is in close contact with the EsaI helix III revealing the distinct differences between the [EsaI.3-oxoC6iACP] and [EsaI.3-oxoC8iACP] complexes. B) Binding interfaces of apo, native and non-native cargo-loaded ACPs to BmaI1. In the [BmaI1.C8iACP] complex, the engagement of ACP helix III with enzyme helix I/loop2 and ACP helix II with enzyme helix V / β8 forms the basis of the extended contact between the carrier protein and BmaI1. Additionally, locking the ACP helices to the enzyme provides a trajectory for flipping C8 cargo from the ACP pocket to the acyl-chain binding pocket in the enzyme. The docked pose in the less productive [BmaI1.3-oxoC8iACP] and [BmaI1.C6iACP] are similar, revealing the nature of the catalytically less competent ES complexes in BmaI1 catalysis.

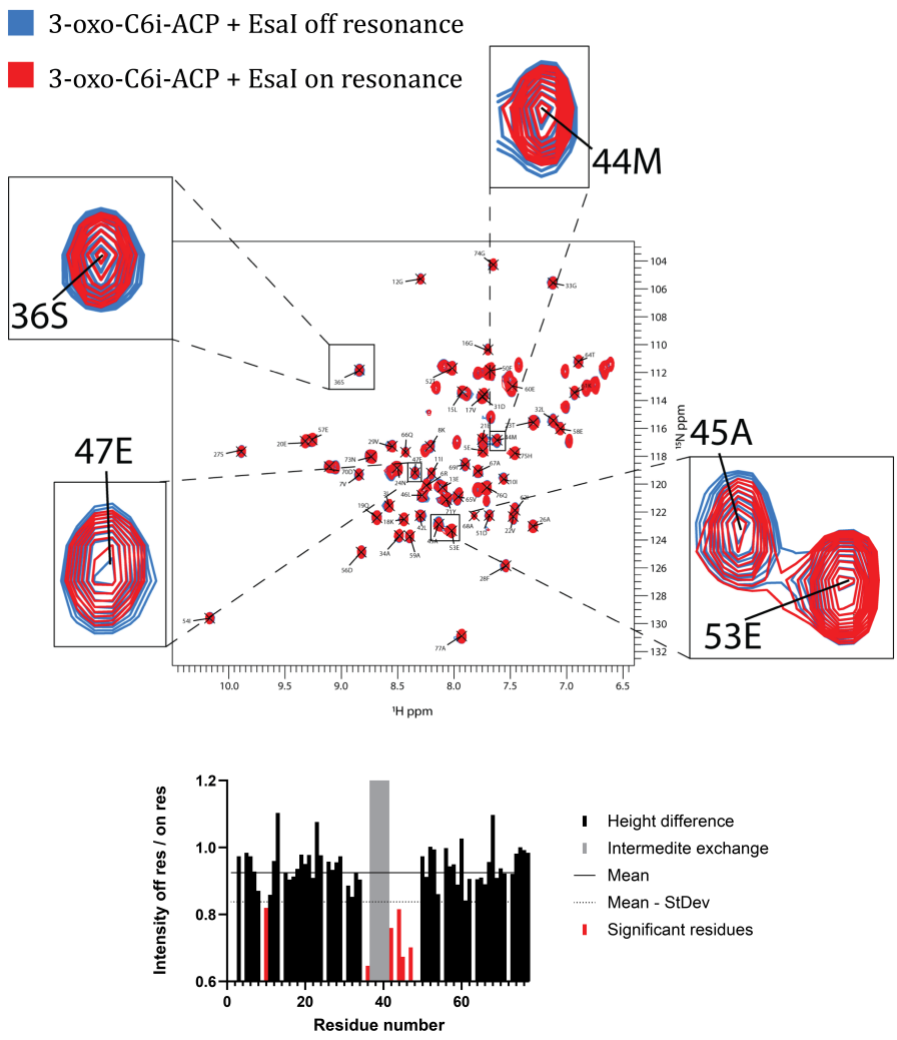

Figure S16. CST experiments of 3-oxo-C6i ACP and EsaI.
U-^{15}N-^{2}H 3-oxo-C6i ACP (100 µM) and unlabeled EsaI (150 µM) were combined, and CST experiments were recorded on-resonance with respect to the chemical shift of EsaI methyl protons (red) and off-resonance (blue). The difference in peak intensity was plotted as a function of residue number to analysis proximity of ACP backbone NH resonances to EsaI. The analysis shows intensity reduction restricted to helix two (residues ~36-48). The intensity reduction does not extend to the C-terminus of the protein (see zoom in on AA 45A and 53E), therefore concluding that CSPs observed in titration experiments at the C-terminus are likely due to conformational changes and not direct binding events.

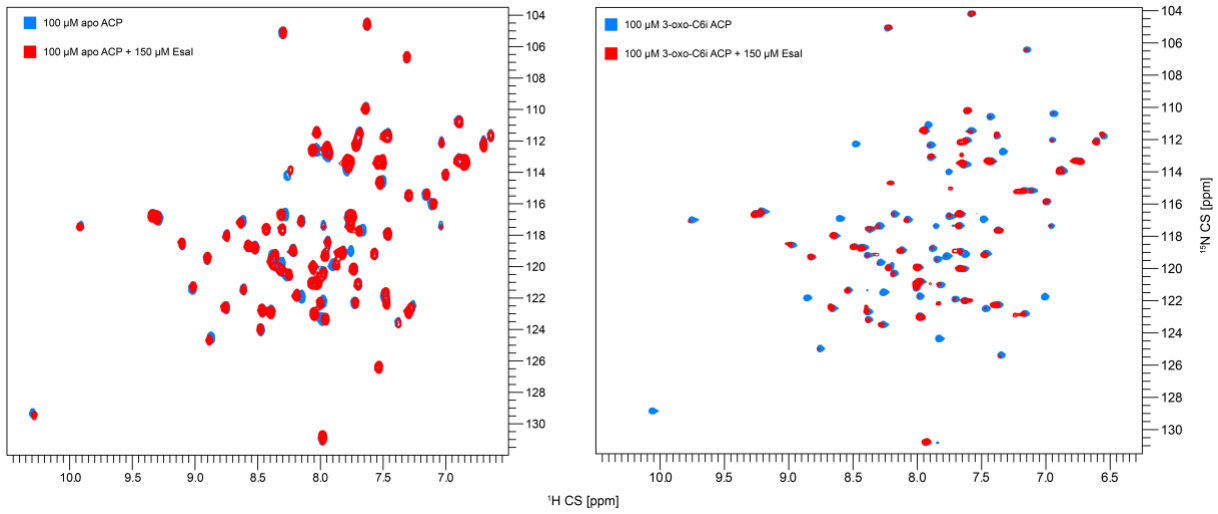

Figure S17. CSP/Intensity comparison between apo-ACP/EsaI and 3-oxo-C6i ACP/EsaI
Left :- Comparison of ^{15}N-^{1}H HSQC of apo ACP with (red) and without (blue) unlabeled EsaI and Right:- native 3-oxo-C6i ACP alone (blue) and in complex with EsaI complex (right). We observe enhanced CSPs and/or reduction in intensity of the ACP signals when the appropriate cargo is loaded suggestive of a tighter interaction.

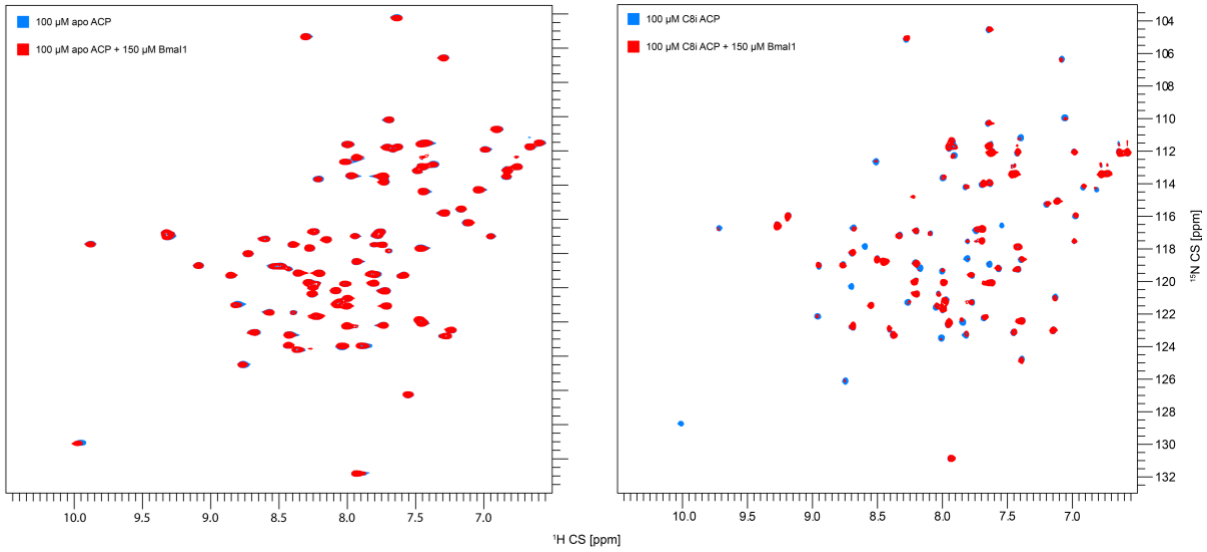

Figure S18. CSP/Intensity comparison between apo-ACP/BmaI1 and C8i ACP/BmaI1
Left :- Comparison of apo ACP (blue) after addition of BmaI1 (red) and Right:- the native C8i ACP alone (blue) and in complex with BmaI1(red). We observe enhanced CSPs and/or reduction in intensity of the ACP signals when the appropriate cargo is loaded suggestive of a tighter interaction.

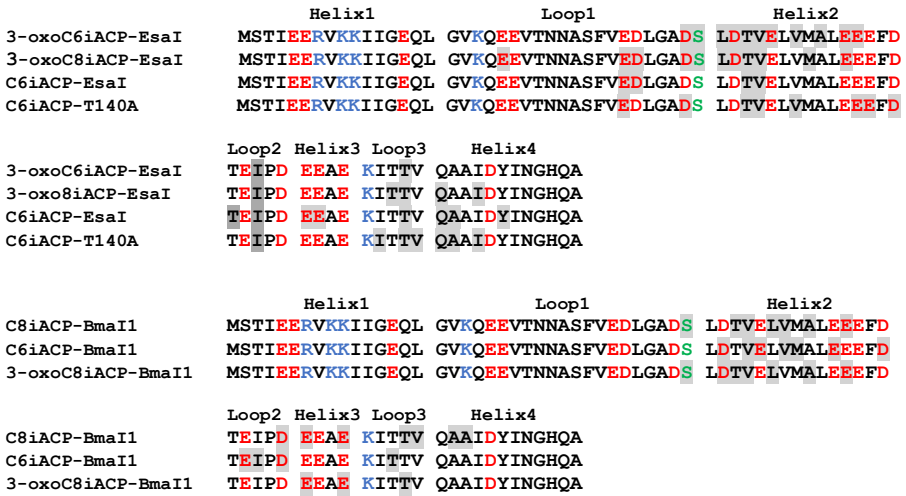

Figure S19 Chemical shift perturbation analysis of native and non-native alkyl-ACPs bound to EsaI and BmaI1.

Acidic basic and the phosphopantetheinylated serine (S36) residues are colored, respectively, in red, blue and green. Residues undergoing significant CSPs/intensity reductions are shaded in gray.

C6i ACP

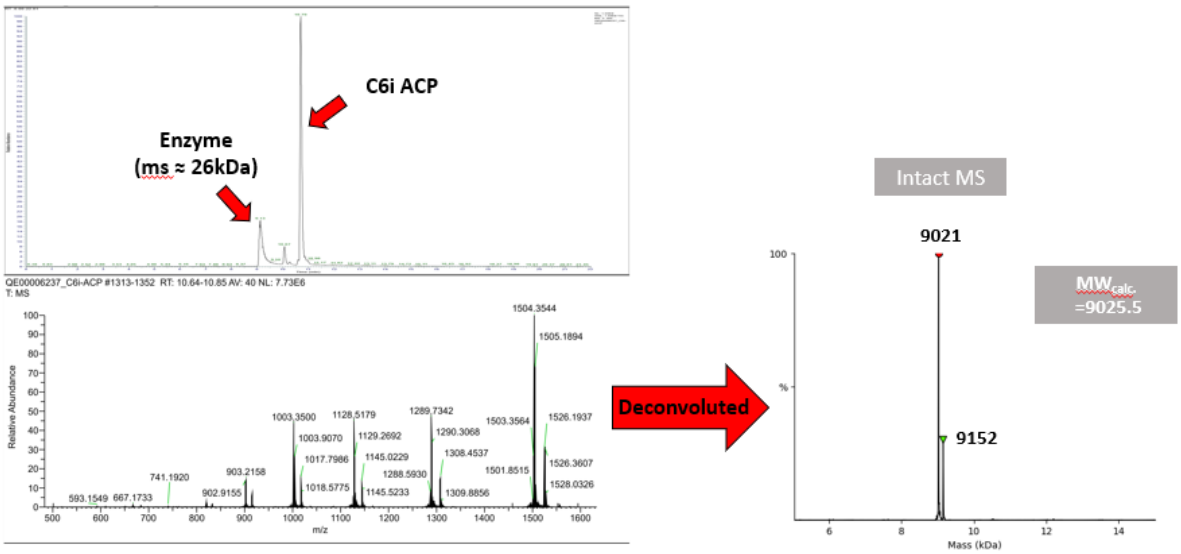

Figure S20. Intact mass spectrometry analysis of C6i ACP. The calculated mass ($MW_{calc.}$) is based on 100% ^{15}N-labeled protein. Assuming labeling efficiency of 96% ^{15}N incorporation, the expected mass would be 9021.1 Da.

C8i ACP

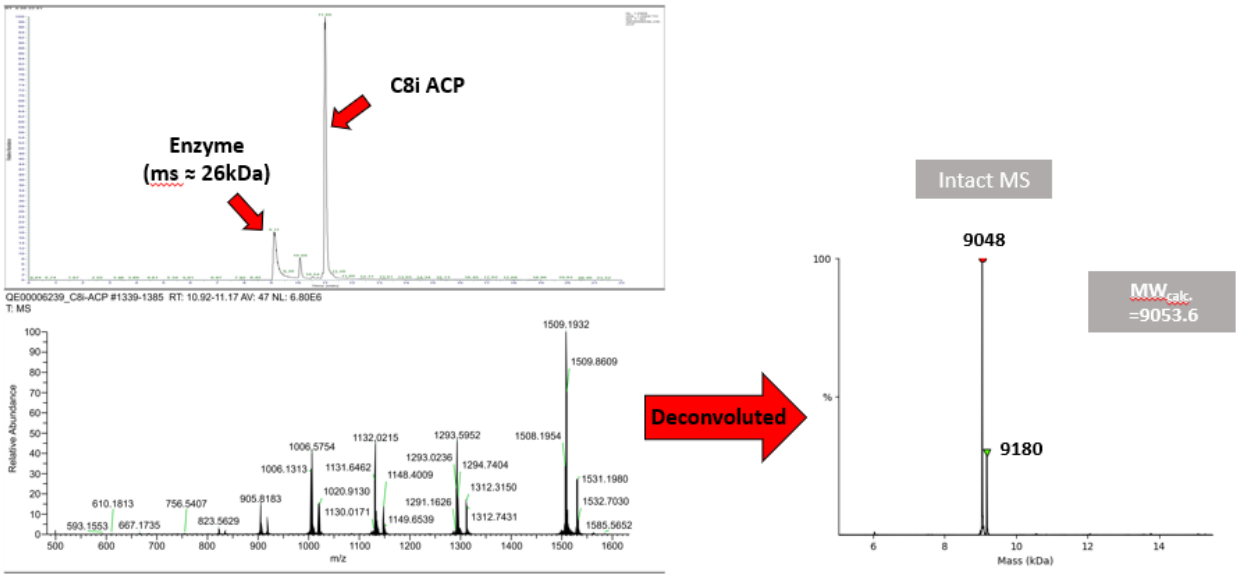

Figure S21. Intact mass spectrometry analysis of C8i ACP. The calculated mass ($MW_{calc.}$) is based on 100% ^{15}N-labeled protein. Assuming labeling efficiency of 96% ^{15}N incorporation, the expected mass would be 9049.1 Da.

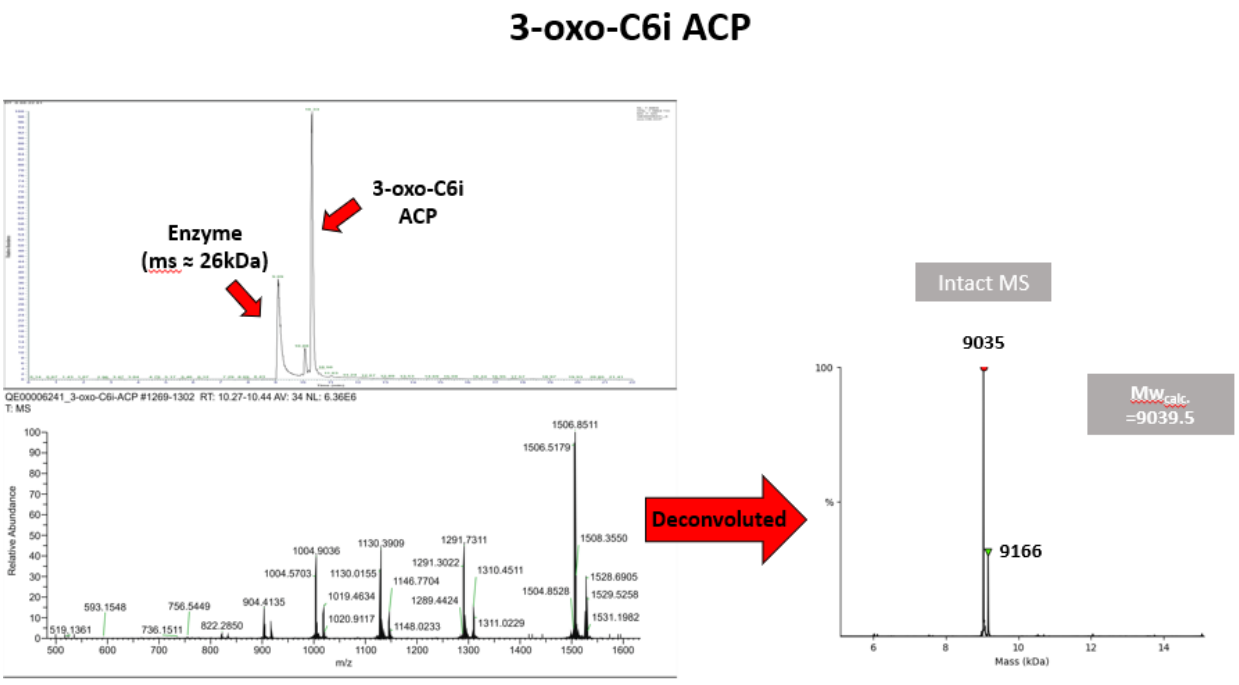

Figure S22. Intact mass spectrometry analysis of 3-oxo-C6i ACP. The calculated mass ($MW_{calc.}$) is based on 100% ^{15}N-labeled protein. Assuming labeling efficiency of 96% ^{15}N incorporation, the expected mass would be 9035.1 Da.

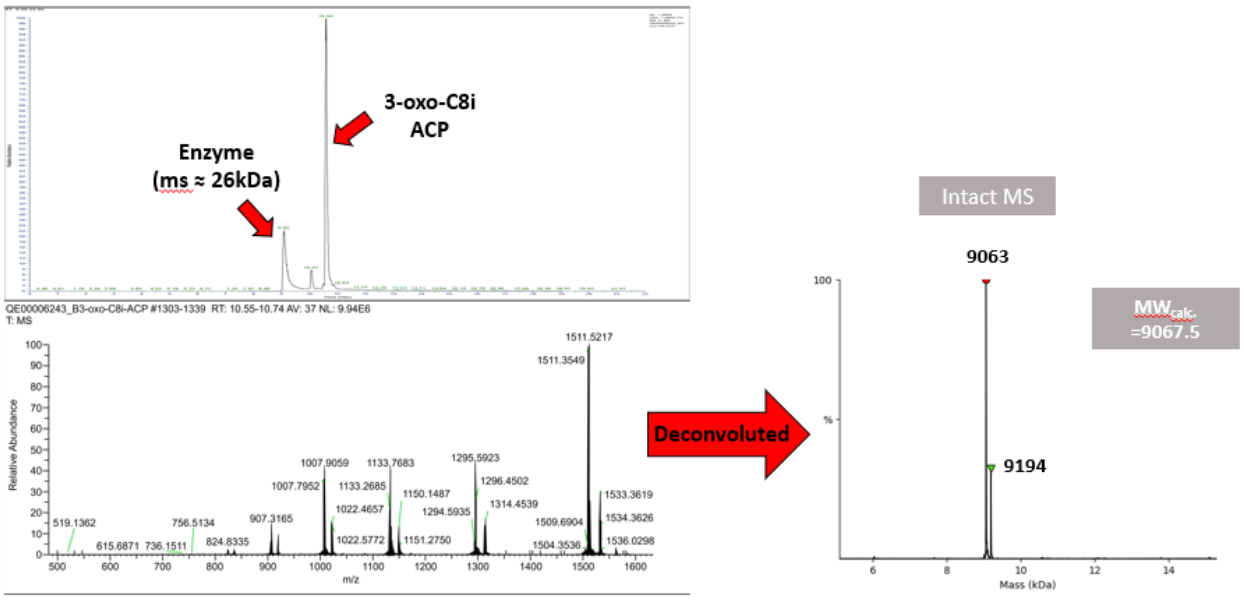

Figure S23. Intact mass spectrometry analysis of 3-oxo-C8i ACP. The calculated mass ($MW_{calc.}$) is based on 100% ^{15}N-labeled protein. Assuming labeling efficiency of 96% ^{15}N incorporation, the expected mass would be 9063.1 Da.

Table S1. Kinetic constants of EsaI and BmaI1 substrates

Substrate	Enzyme	K_m (μM)	k_{cat} (min^{-1})	k_{cat}/K_m x 10^{-2} (μM^{-1} min^{-1})
Furanacetyl-ACP[a]	EsaI	10.8 ± 1.42	3.99 ± 0.14	37 ± 5
Benzofuranacetyl-ACP[a]	EsaI	16.6 ± 1.88	0.84 ± 0.02	5.1 ± 0.6
C6-ACP	EsaI	61.9 ± 7.69	0.51± 0.02	0.83 ± 0.11
C6-ACP	EsaI T140A	3.08 ± 0.33	1.56 ± 0.04	51 ± 6
C8-ACP	BmaI1	6 ± 1	5.76 ± 0.60	96 ± 18
C6-ACP	BmaI1	4 ± 1	1.50 ± 0.12	38 ± 10

[a] Furanacetyl-ACP and Benzofuranacetyl-ACPs, respectively, are 3-oxoC6-ACP and 3-oxoC8-ACP substrate mimics. With the exception of benzofuranacetyl-ACP, the kinetic constants for the substrates are adopted from references 7 and 8.

References

[1] N. Azizi, A. K. Amiri, M. Bolourtchian and M. R. Saidi, *J. Iran. Chem. Soc.*, 2009, **6**, 749.

[2] J. S. Yadav, T. Swamy, B.V. S. Reddy, D. K. Rao *Journal of Molecular Catalysis A: Chemical* 2007, **274**, 116.

[3] F. M. da Silva and J. Jones Jr, *J. Braz. Chem. Soc.*, 2001, **12**, 135.

[4] J.E. Cronan, J. Thomas, In *Complex Enzymes in Microbial Natural Product Biosynthesis, Part B: Polyketides, Aminocoumarins and Carbohydrates*, 2009, **17**, 395.

[5] D. H. Keating, M.R. Carey, J. E. Cronan, *J. Biol. Chem.* 1995, **270** , 22229.

[6] S. Jackowski, *Journal of Bacteriology* 1981, **148**, 926.

[7] A. N. Montebello, R. M. Brecht, R. D. Turner, M. Ghali, X. Pu, R. Nagarajan, *Biochemistry* 2014, **53**, 6231

[8] M. N. Lam, D. Dudekula, B. Durham, N. Collingwood, E. C. Brown, R. Nagarajan, Chem. Commun., 2018, **54**, 8838.

[9] L. E. Quadri, P. H. Weinreb, M. Lei, M. M. Nakano, P. Zuber, C. T. Walsh, (1998) *Biochemistry*, 1998, **37**, 1585.

[10] N. M. Kosa, R. W. Haushalter, A. R. Smith, M. D. Burkart, Nat. Methods, 2012, **9**, 981.

[11] S. G. Hyberts, K. Takeuchi, G. Wagner, *J Am Chem Soc* 2010, **132**, 2145.

[12] S. G. Hyberts, A. G. Milbradt, A. B. Wagner, H. Arthanari, G. Wagner, *J Biomol NMR* 2012, **52**, 315.

[13] F. Delaglio, S. Grzesiek, G. W. Vuister, G. Zhu, J. Pfeifer, A. Bax, *Journal of Biomolecular NMR* 1995, **6**, 277.

[14] W. F. Vranken, W. Boucher, T. J. Stevens, R. H. Fogh, A. Pajon, M. Llinas, E. L. Ulrich, J. L. Markley, J. Ionides, E. D. Laue, *Proteins* 2005, **59**, 687.

[15] ProMod3—A versatile homology modelling toolbox, (available at https://journals.plos.org/ploscompbiol/article?id=10.1371/journal.pcbi.1008667).

[16] ICM—A new method for protein modeling and design: Applications to docking and structure prediction from the distorted native conformation - Abagyan - 1994 - Journal of Computational Chemistry - Wiley Online Library, (available at https://onlinelibrary.wiley.com/doi/abs/10.1002/jcc.540150503).

[17] T. G. Bartholow, T. Sztain, A. Patel, D. J. Lee, M. A. Young, R. Abagyan, M. D. Burkart,. *Communications Biology*, 2021, **4**, 340.

[18] Y. A. Arnautova, R. A. Abagyan, M. Totrov, *Proteins*. 2011, **79**, 477.

[19] T. Sztain, T. G. Bartholow, D. J. Lee, L. Casalino, A. Mitchell, M. A. Young, J. Wang, J. A. McCammon, M. D. Burkart, Proc. Natl. Acad. Sci. USA, 2021, 118, e2025597118.

[20] Schrodinger, LLC, *The PyMOL Molecular Graphics System*.

[21] M. A. C. Neves, M. Totrov, R. Abagyan, D *J. Comput. Aided Mol. Des.* 2012, **26**, 675.

[22] Frank Delaglio, Stephan Grzesiek, Geerten. W. Vuister, Guang Zhu, John. Pfeifer, and Ad Bax, NMRPipe: a multidimensional spectral processing system based on UNIX pipes, *J. Biomol. NMR.* 6, 277-293 (1995).

[23] W. F. Vranken, W. Boucher, T. J. Stevens, R. H. Fogh, A. Pajon, M. Llinas, E. L. Ulrich, J. L.Markley, J. lonides, E. D. Laue, The CCPN data model for NMR spectroscopy: Development of a software pipeline. *Proteins Struct. Funct. Bioinforma.* 2005, 59, 687- 696.

[24] Shimada I (2005) NMR techniques for identifying the interface of a larger protein-protein complex: cross-saturation and transferred cross-saturation experiments, *Methods in Enzymology* 394:483–506.

[25] Wüthrich K (2000) Protein recognition by NMR, *Nature Structural Biology* 7:188–189.

[26] Takahashi H, Nakanishi T, Kami K, Arata YShimada I (2000) A novel NMR method for determining the interfaces of large protein-protein complexes, *Nature Structural Biology* 7:220–223.